Environmental and Systemic Exposure Assessment for Green Sturgeon Following Application of Imidacloprid for the Control of Burrowing Shrimp in Willapa Bay, Washington

John A. Frew

A dissertation

submitted in partial fulfillment of the

requirements for the degree of

Doctor of Philosophy

University of Washington

2013

Reading Committee:

Christian Grue, Chair

John Nichols

Graham Young

Program Authorized to Offer Degree:

School of Aquatic and Fishery Sciences

University of Washington

Abstract

Environmental and Systemic Exposure Assessment for Green Sturgeon Following Application of Imidacloprid for the Control of Burrowing Shrimp in Willapa Bay, Washington

John A. Frew

Chair of the Supervisory Committee:
Christian E. Grue, Associate Professor
School of Aquatic and Fishery Sciences

The neonicotinoid insecticide imidacloprid (IMI) has been proposed for the control of burrowing shrimp on oyster beds in Willapa Bay, Washington. Use of IMI may be denied if it is shown that ESA-listed green sturgeon are adversely affected as a result of exposure to the compound. Green sturgeon were found to feed opportunistically on IMI-impaired shrimp following test applications of the insecticide. Foraging activities could result in exposure to IMI in sediment pore water and from the consumption of contaminated shrimp. An exposure characterization revealed maximum IMI residue concentrations of 27.8 μg L^{-1} in pore water and 31.4 μg kg^{-1} in shrimp. Results from modeling branchial and dietary uptake indicated that pore water exposure would account for most of the systemic absorption of IMI. The 96-h median lethal toxicity (LC_{50}) for surrogate juvenile white sturgeon was 124 mg L^{-1}, indicating sturgeon do not possess

extreme sensitivity to IMI. Controlled exposures to white sturgeon of maximum IMI field concentrations did not result in overt effects, but showed relatively long persistence of the chemical in plasma. Toxicokinetic studies were conducted with rainbow trout (RBT) to describe the disposition and elimination of IMI in fish. Results suggest no dose-dependence on kinetics following interarterial bolus injections of a low (44.7 μg kg^{-1}) or high (250.0 μg kg^{-1}) dose of IMI. Mean values for the steady-state volume of distribution (V_{ss}) were 1561.9 and 1922.5 mL kg^{-1} for the low and high dose groups, respectively. Mean whole body clearance (CL_B) was 20.5 mL h^{-1} kg^{-1} for both groups. The elimination half-life ($t_{1/2}$) was 65.6 and 68.2 h for the low and high dose groups, respectively. Mass-balance analysis revealed that branchial clearance accounted for almost 50% of CL_B. Measured tissue:plasma IMI residue concentration ratios in RBT and white sturgeon were comparable, suggesting that both species handle the chemical in a similar manner. The hazard quotient (HQ), the ratio of the maximum pore water concentration over the LC_{50} value, was two orders of magnitude below the threshold for potential effects. This implies that green sturgeon would be at minimal risk from exposure to IMI in Willapa Bay.

Environmental and Systemic Exposure Assessment for Green Sturgeon Following Application of Imidacloprid for the Control of Burrowing Shrimp in Willapa Bay, Washington

INTRODUCTION

Pesticide registration and the Endangered Species Act

Under the Federal Insecticide, Fungicide and Rodenticide Act (FIFRA), registration for the use of pesticides is under the authority of the US Environmental Protection Agency (USEPA). Prior to granting a registration, applicants must demonstrate to the USEPA that the pesticide does not cause unreasonable adverse environmental effects. The Endangered Species Act (ESA) was enacted to identify species whose populations are threatened or endangered and effect the protections necessary for recovery. The US Fish and Wildlife Service (USFWS) and National Marine Fisheries Service (NMFS) have the authority to designate or "list" such species. When reviewing a pesticide for registration, the USEPA must evaluate the potential effect from its use on listed species. This may require consultation with USFWS and NMFS to determine the likelihood that use of the pesticide would imperil the listed species. Registration may not be granted if it is shown that direct or indirect adverse effects will result following exposure to the compound [1, 2].

Green sturgeon

The green sturgeon (*Acipenser medirostris*) is an anadromous species ranging along the West Coast of North America from Mexico to Alaska. It is the most marine-oriented of sturgeon species: juveniles spend 1-4 years in freshwater before migrating to sea. Individuals reach sexual maturity at 13-20 years of age, and can live up to 70 years [3, 4]. Following sexual maturity, they return to their natal rivers to spawn every 2-5 years [4].

Two genetically distinct population segments (DPSs) have been identified: the northern DPS, comprising spawning populations in the Rogue River of southern Oregon and the Klamath River in northern California / southern Oregon, and the southern DPS originating solely from the Sacramento River in California [5]. The southern DPS was listed as "threatened" under the ESA in 2006 due to multiple threats resulting in a decrease in population numbers including loss of spawning habitat, and reduced growth and survival as a result of increased water temperatures, entrainment by water diversions, exposure to contaminants, competition from exotic species, and loss as bycatch in commercial fish harvests, [4, 6].

Critical habitat was established for the southern DPS in 2009. This protective designation extends throughout the freshwater, estuarine, coastal, and marine areas commonly occupied by green sturgeon, including the Sacramento River and major tributaries downstream of impassible dams, and all marine waters – inclusive of estuaries and the coast – up to 110 m depth from Monterey Bay to the US–Canada border. This designation provides protection against activities that could adversely affect green sturgeon [7]. Primary constituent elements (PCEs) – essential requirements for conservation of the southern DPS – were identified for the general areas comprising the critical habitat. Ensuring the normal behavior, growth and survival of the southern DPS, the PCEs recognized for estuaries include maintenance of abundant food resources as well as suitable water and sediment quality [7].

Willapa Bay and Grays Harbor

The Willapa Bay and Grays Harbor estuaries in Washington State are within the designated critical habitat. Combined, also they comprise the largest oyster-growing region on the Pacific Coast, accounting for over 60% of the total oyster harvest in Washington State [8]. Pacific

oysters (*Crassostrea gigas*) are cultivated on the intertidal mud flats. The most widely used production process involves seeding hatchery-grown oyster larvae onto crop beds. The oysters are then harvested after 2-4 years of maturation [9].

The presence of two species of indigenous burrowing shrimp on the mud flats, the ghost shrimp (*Neotrypaea californiensis*) and the mud shrimp (*Upogebia pugettensis*), impedes the success of rearing oysters [8, 9]. Burrows created by these shrimp disrupt the sediments and reduce their compaction. Oyster larvae suffer decreased growth and potential suffocation from bioturbation of the sediments, and death from burial within the destabilized mud. These factors drastically reduce the value of the oyster harvest [8, 9].

Since 1963, the carbamate insecticide carbaryl (1-napthyl n-methyl carbamate) has been applied to oyster beds at low tide for the control of burrowing shrimp. The direct application of this insecticide in an aquatic environment has created controversy in part because of concerns about potential impacts to non-target species [8-10]. Dispute over the use of carbaryl prompted a legal settlement in 2001 between the Willapa and Grays Harbor Oyster Growers Association (WGHOGA) and the Washington Toxics Coalition. This required annual reductions in treated acreage and the discontinuation of carbaryl applications in 2012. The settlement also established an integrated pest management (IPM) program focused on finding an alternative to carbaryl for the control of burrowing shrimp.

Imidacloprid

The insecticide imidacloprid (IMI), IUPAC name N-[1-[(6-chloropyridyn-3-yl)methyl]-4,5-dyhydroimidazol-2-yl]nitramide, has been identified as an alternative to carbaryl for the control of burrowing shrimp [11]. IMI is a member of the class of compounds called neonicotinoids –

insecticides possessing a mode of action modeled after the plant toxin nicotine [12]. First registered for use in the United States in 1992, IMI is the most widely used neonicotinoid and has the fastest growth in sales of any insecticide [12].

IMI is approximately two orders of magnitude less toxic to fish than carbaryl. The median lethal concentration (LC_{50}) for juvenile rainbow trout (*Oncorhynchus mykiss* – RBT) in static 96-h acute toxicity tests is 211 mg L^{-1} for IMI, compared with 4.38 mg L^{-1} for carbaryl [13, 14]. Additionally, the proposed application rate for IMI is approximately $1/16^{th}$ that of carbaryl: 0.56 kg ha^{-1} (0.5 lb ac^{-1}) active ingredient (a.i.) IMI vs. 8.9 kg ha^{-1} (8.0 lb ac^{-1}) a.i. carbaryl (K Patten, Washington State University, Long Beach, WA, personal communication).

IMI is a neurotoxicant that acts as an agonist at the acetylcholine (ACh) binding sites on nicotinic acetylcholine receptors (nAChRs), but does not act on muscarinic acetylcholine receptors (mAChRs) [15]. The binding of IMI on a post-synaptic nAChR results in the opening of the receptor, creating a channel for Na^+ ions to enter the post-synaptic neuron and propagate a nerve signal. The nAChR can be desensitized from over-stimulation caused by the binding of IMI, resulting in the closing of the receptor and prevention of all nerve signal transmission. Desensitization of enough receptors may ultimately result in death of the exposed organism [16].

Structurally, IMI consists of two parts: a 6-Chloro-3-pyridyl moiety resembling nicotine, and a 2-nitroimino-imidazolidine (nitroguanidine) group [12]. The electronegative nitroguanidine group has been identified as the pharmacophore [16, 17]. IMI is a relatively small compound (molecular weight = 255.7 g mol^{-1}). It is moderately polar, with an octanol/water partition coefficient (K_{ow}) of 3.72 ($\log K_{ow} = 0.57$) [18]. IMI is barely ionized at physiological pH (it is not possible to specify its pK_a in pure aqueous systems) [19]. Its water solubility is independent

of pH over a large range. The measured value at 20 °C between pH 4.0 and 9.0 is 610 mg L^{-1} [18].

Potential exposure of green sturgeon to IMI

Sexually mature and immature adult green sturgeon from both DPSs occupy Willapa Bay and Grays Harbor during summer and early fall [20]. Based on mixed stock analysis of green sturgeon examined in Washington coastal areas, it is estimated that both groups are evenly represented in Grays Harbor while Willapa Bay is populated principally by the southern DPS [5, 21]. An investigation of stomach contents of green sturgeon caught as bycatch in Willapa Bay revealed that fish fed on burrowing shrimp [20, 21]. Additionally, the presence of feeding pits – shallow depressions on the mudflats – throughout the Bay has been linked to predation on burrowing shrimp by green sturgeon. It has been proposed that these fish move onto the beds during high tide. Through the use of specially adapted sensory organs called Ampullae of Lorenzini, green sturgeon are able to locate burrowing shrimp by sensing electrical signals given off by the organisms [22]. They then dig and suck the detected shrimp out of their burrows, leaving the feeding pits as evidence of their predation [20, 21].

There have been accounts of an increase in the number of feeding pits following test applications of IMI on intertidal beds densely populated with burrowing shrimp (K Patten, Washington State University, Long Beach, WA, personal communication). This may be indicative of preferential feeding on exposed shrimp by green sturgeon. Observations of shrimp exposed to IMI in the field and in controlled tests at the University of Washington (UW, C.E. Grue and co-workers, unpublished data) revealed a long period of impairment, characterized by involuntary muscle spasms and an inability to move to lower depths in their burrows, prior to

death. Opportunistic sturgeon may be cuing in on these distressed shrimp, thereby becoming exposed to IMI in sediment pore water and the bodies of their prey. The potential exposure of the southern DPS to IMI could impede the protective measures established under the ESA listing [1, 6, 7]. Under the green sturgeon final 4(d) rule, Federal registration and State permitting approval for IMI may be denied if it is shown that direct or indirect adverse effects will result from use of the compound [1].

Sources and routes of exposure

IMI would be applied directly on oyster-rearing mudflats at low tide in Willapa Bay and Grays Harbor. Efficacy for controlling burrowing shrimp would be dependent on adequate concentrations of the chemical leaching into sediment pore water following surface applications. Chemical remaining on the surface would be rapidly diluted in the water column following tidal inundation. These low and ephemeral concentrations of IMI in the water column likely would not provide a significant source of exposure for green sturgeon. Concentrations of IMI in sediment pore water may be more persistent, however. Green sturgeon feeding on burrowing shrimp may incur exposure to IMI via two pathways: diffusion of the compound from the pore water, and through the consumption of contaminated shrimp. Based on their feeding behavior along with the physicochemical properties of IMI (i.e., low molecular weight and predominantly neutral at environmental and physiological pH), the potential for systemic absorption exists via diffusion of the chemical across the gills and/or the gastrointestinal tract (GIT) [23, 24]. Transport of IMI across the skin likely would be relatively minor compared with the other absorption routes [25].

Goals

The goals of this study were to evaluate the likelihood that green sturgeon would be exposed to IMI, characterize the environmental exposure, describe the disposition of the chemical following uptake, and assess the potential for direct adverse effects.

Objectives

1. Detection protocol and sample preparation optimization

IMI residues were quantitated in different matrices. A protocol for LC-MS/MS detection was optimized for application across all sample mediums. Sample preparation methods incorporating ultrasonic dismembration were adapted and optimized. An enzyme-linked immunosorbent assay (ELISA) was optimized for quantification of IMI residues in plasma. The assay would be applied for low-cost, high-throughput screening of samples following green sturgeon environmental monitoring, as discussed below.

2. Toxicity of derivatives

A literature review was conducted for the identification of IMI derivatives formed as a result of environmental degradation. An assessment was made of the potential toxicity of these breakdown products to green sturgeon relative to IMI in order to determine whether any warranted examination along with the parent compound.

3. Confirmation of opportunistic feeding

An investigation was conducted to determine whether green sturgeon feed preferentially on IMI-impaired shrimp, thereby increasing the likelihood of exposure to the chemical. New

sturgeon pits were counted on IMI-treated and non-treated (control) beds daily following application of the chemical. Opportunistic feeding was determined by comparing the difference in the number of pits pre- and post-application on both bed types: a significantly greater number of new pits on the treatment beds would be indicative of IMI-induced preferential feeding.

4. Exposure characterization

Sediment pore water and burrowing shrimp were identified as the major sources of IMI exposure to green sturgeon. In order to determine the levels at which sturgeon could be exposed, IMI residues were quantified in samples collected at successive time intervals at multiple locations in both mediums following application of the chemical on test beds in Willapa Bay. Bed and sediment characteristics vary among locations throughout the Bay. These features affect the amount of IMI that is successfully incorporated into the sediment pore water. Bed and sediment characteristics were described for the test and control sampling locations. Worst-case exposures were modeled at peak IMI residue concentrations in pore water and shrimp encountered by sturgeon foraging on the beds.

5. *Exposure verification*

Green sturgeon were sampled in an environmental monitoring effort following application of IMI in an attempt to confirm environmental exposure. Blood samples were collected from green sturgeon for determination of exposure by quantification of IMI residues in plasma using LC-MS/MS detection.

6. Uptake estimation

Branchial and dietary uptake models were utilized to estimate the contribution from each route of exposure to overall IMI uptake. Branchial uptake was estimated by factoring in the average IMI pore water concentration at the time of feeding along with the duration of the exposure. Dietary uptake was approximated by multiplying the average amount of IMI residue (the product of average concentration and average mass) per shrimp by the estimated average number of shrimp consumed per sturgeon at each feeding interval.

7. *White sturgeon controlled exposure studies*

The ESA-listing of green sturgeon prevented their use in toxicity studies [6]. Juvenile white sturgeon (*Acipenser transmontanus*) were used as surrogates in controlled IMI exposures. Laboratory toxicity studies were conducted to address the following:

(a). Sturgeon sensitivity to IMI. A 96-h median lethal toxicity (LC_{50}) test was conducted to determine whether sturgeon demonstrate extreme sensitivity to IMI relative to standard test species such as RBT [13].

(b). Simulated field exposures and plasma residue concentrations. Fish were exposed to IMI under conditions (concentrations and durations) simulating expected worst-case scenarios in the field. Preliminary data on the potential levels of exposure indicated that such worst-case scenarios would not result in any overt effects (e.g., lethargy or mortality). IMI residue concentrations measured in plasma were therefore used to provide benchmarks for environmental monitoring. These residue concentrations will serve as an expected ceiling in samples measured from sturgeon in the field post-application.

(c). Persistence of IMI in sturgeon. An assessment was made of the bioaccumulation potential of IMI in sturgeon. It was unknown how long it would take for sturgeon to eliminate IMI from their bodies. A depuration study using white sturgeon in static water-borne exposures to IMI was conducted to determine the blood plasma and tissue half-lives ($t_{½}$) – the time for the chemical concentration to fall by one half. Based on the physicochemical properties of the compound, the working hypothesis was that elimination of IMI would be relatively rapid, with low potential for bioaccumulation [26, 27]. Comparatively short plasma and tissue half-lives had been measured previously in mice [28]. Rats eliminated 96% of an oral dose of IMI within 48 h [29, 30]. No published kinetic studies on IMI in fish were available.

8. Rainbow trout toxicokinetics studies

Bolus dose intra-arterial (i.a.) IMI injections were administered to RBT in a depuration study to obtain further knowledge of IMI disposition in fish. A toxicokinetic (TK) profile based on measured IMI concentrations in plasma was developed to calculate the primary TK parameters whole body clearance (*CL*), volume of distribution (*V*) and total systemic exposure, described as the area under the concentration-time curve (*AUC*). The goal of this effort was to obtain greater insight into the accumulation potential of the chemical along with its persistence within the body of fish. Additional clearance values were calculated from IMI residues quantitated in expired water, bile and urine, and compared with whole body clearance for a mass-balance approximation (i.e., the contribution of each clearance source to overall whole body clearance). This was used to illustrate the significance of these routes to overall clearance of IMI in fish.

9. Hepatic metabolism study

A preliminary hepatic metabolism study was undertaken in support of the mass-balance analysis discussed above. Extensive IMI metabolism has been measured in human and rodent liver microsomes and rabbit liver cytosol [28, 31-35]. The capability of hepatic metabolism of IMI in fish was unknown, however. Hepatic biotransformation of IMI was examined utilizing a substrate depletion assay with RBT liver S9 fractions. The hypothesis was that hepatic metabolism, as measured by decreases of IMI in the RBT S9 fractions, would be observed. This hypothesis was supported by the aforementioned evidence of hepatic biotransformation in other species, and the presence of the same cytochrome P450 (CYP) isoforms in RBT that are known to metabolize IMI in humans [31, 34, 35].

MATERIALS AND METHODS

1. Detection protocol and sample preparation optimization

(a). LC-MS/MS quantitation

IMI residues were quantitated using high performance liquid chromatography tandem mass spectrometry (LC-MS/MS) detection through adaptation of an existing protocol [36]. This method was used for quantification of IMI in all of the sample matrices. Method utilization and optimization followed USEPA-specified guidelines [37]. LC-MS/MS conditions and instrumentation were as follows:

- HPLC instrument: 2795 Alliance HT – quaternary system (Waters Corp.)[1]

[1] Mention of products and supplies is for identification purposes only and does not constitute endorsement by the author or the agencies with which the author was affiliated during the conduct of these studies.

- Column: HPLC Zorbax SB-C18 narrow bore RR 2.1 x 100 mm 3.5-Micron (Agilent Technologies, Inc.)
- Injection volume: 10 μL
- Oven temperature: 30 °C
- Mobile phase A: de-ionized (DI) water, 5% acetonitrile (ACN), 1% acetic acid
- Mobile phase B: 99% ACN, 1% acetic acid
- Mobile phase C: isopropanol (IPA)
- Detector: Quattro Micro triple quadrapole LC-MS/MS mass spectrometer (Waters Corp.)
- Interface: electrospray, +5000 V turbo ion spray potential, 300 °C temperature
- Scan type: MRM (multiple reaction monitoring mode)
- Polarity: positive
- Collision gas: argon

A deuterium-labeled internal standard (IS – Fluka Pestanal® Imidacloprid-d_4, Sigma-Aldrich) was incorporated into the samples for positive control validation. IMI ions containing the two principal stable chlorine isotopes (^{35}Cl and ^{37}Cl) have masses of 256 (IMI-35) and 258 (IMI-37) amu, respectively. The IS, with deuterium isotopes replacing four hydrogen atoms on the pyridinyl ring, have masses of 260 for the ^{35}Cl (IS-35) and 262 for the ^{37}Cl (IS-37) amu (Fig. 1). Two MS/MS transitions were recorded for both the parent and IS: 209 (IMI 35) and 211 (IMI 37) amu; and 213 (IS 35) and 215 (IS 37) amu.

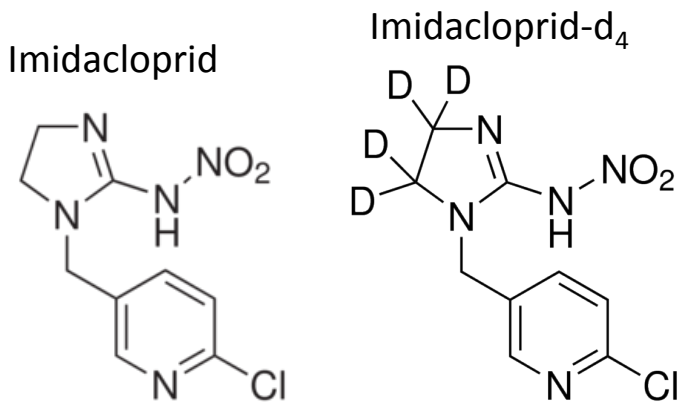

Fig. 1. Imidacloprid (IMI) and Imidacloprid-d4 internal standard (IS).

Calibration standards were created for the development of a standard curve for use on each LC-MS/MS run. IMI calibrators of 1, 10, 100 and 1000 μg L^{-1} were developed in 30:70 ACN/DI water – the approximate starting concentration of the initial mobile phase – using an IMI reference standard (Chem Service, Inc.). IS (50 μg L^{-1}) was incorporated into each of the parent compound standards. Concentrations on the calibration curve were reported as parent : IS area (i.e., mass : charge – m/z) ratios.

Similar to the calibration standards, samples to be analyzed were spiked with IS for a reconstitution volume concentration of 50 μg L^{-1}. Parent : IS ratios were used for calculating the sample concentrations from the derived calibration curve. Due to the near-identical molecular structure of the IS to the parent, retention time and recovery of both compounds following sample preparation and LC-MS/MS detection was expected to be the same.

A partial loop injection of 10 μL of sample was combined with wash solution (50% IPA, 50% methanol – MeOH) and purge solution (10% ACN, 90% water) in the 50 μL HPLC sample loop. The 12-min gradient timetable was as follows: an initial mobile phase of 68% solution A, 32% solution B at a flow rate of 200 μL min^{-1} from time interval 0 – 4.5 min; 52% solution A, 48% solution B, at a flow rate of 200 μL min^{-1} from time interval 4.5 – 6.5 min; 1% solution A,

65% solution B, and 34% solution C at a flow rate of 350 µL min^{-1} from 6.5 – 9.0 min; 32% solution B and 68% solution C at a flow rate of 350 µL min^{-1} from 9.0 – 11.0 min, with the flow rate reduced to 200 µL min^{-1} from 11.0 – 12.0 min. The analyte retention time window was approximately 2.6 – 3.0 min (Fig. 2).

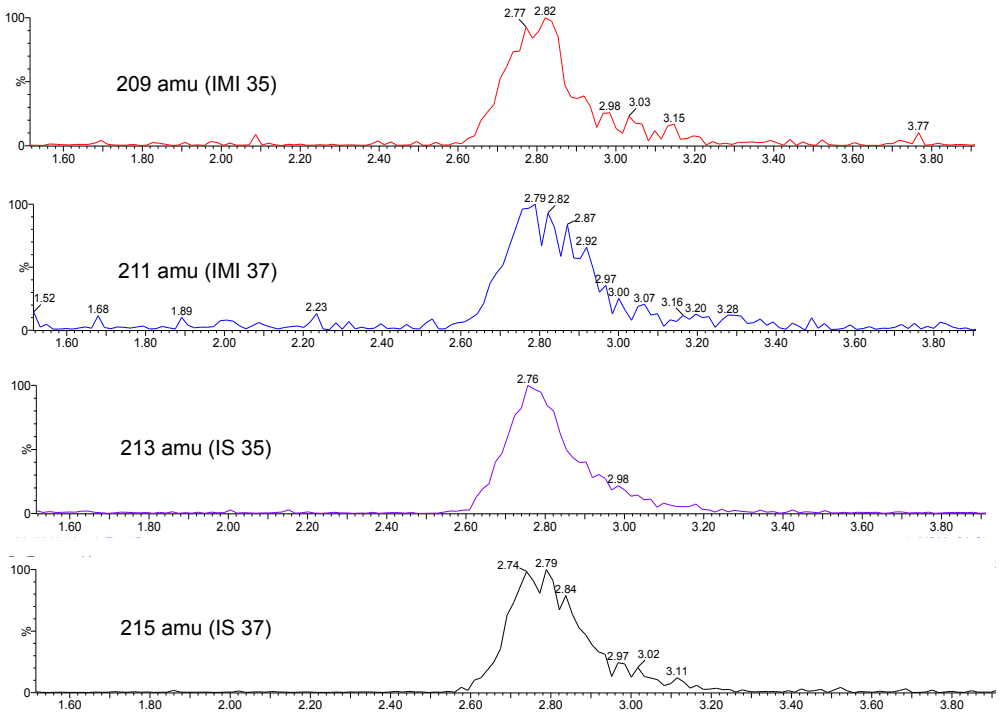

Fig. 2. Peak retention times for imidacloprid (IMI) and internal standard (IS) fragments.

(b). Sample preparation protocols

Sediment pore water. IMI residues were quantitated in pore water extracted from sediment samples collected in Willapa Bay, as described below. The approximately 1500 g sediment samples were enclosed in 1-L containers (Nalgene® Wide-Mouth Bottle, HDPE, Nalge Nunc Int'l.). Samples were mixed in their containers to ensure equal distribution of water throughout the sediment. Approximately 400 g of each homogenate was transferred to a disposable 500-mL,

vacuum filtration unit (Steritop™ Express™ PLUS 0.22 μm, Millipore). Pore water (approximately 5-10 mL, depending on sediment saturation) was extracted under vacuum into clean 50-mL conical tubes. A 2.0 g aliquot from each sample was decanted into 15-mL conical tubes and spiked with 0.05 g of 1000 μg L^{-1} IS. The samples were transferred to 4.0 mL, 200 mg bed weight SPE columns (Grace C_{18} Extract Clean, Grace Division Discovery Sciences) and desalted by reversed phase solid phase extraction (SPE) using a 12-port vacuum manifold (Supelco Visiprep, Sigma-Aldrich) following the manufacturer's recommended protocol. A manifold attachment (Supelco Visidry, Sigma-Aldrich) was used for drying the methanol (MeOH) eluents under N_2. Dried samples were reconstituted in 1.0 g 30:70 acetonitrile (ACN)/DI water for quantitation using LC-MS/MS detection.

Plasma and bile. Sample preparation of plasma and bile was adapted from an established protocol [28]. Plasma (0.025 – 0.125 g) and bile (0.200 – 0.300 g) were transferred to 50-mL conical tubes and 0.0125 or 0.025 g 1000 μg L^{-1} IS, depending on reconstitution volume, was added and allowed to equilibrate in the dark for 2 h at 4 °C. Following equilibration, 5 mL ACN and 250 mg NaCl were added. The samples were placed on ice and homogenized using a sonic dismembrator (Model 4C15, Fisher Scientific) set at maximum power for 2 min., followed by vigorous vortexing for 1 min. The supernatant was collected after centrifugation at 4000 x *g* for 15 min., transferred to a glass evaporation tube, and dried under N_2 in a vacuum manifold. Dried samples were reconstituted in either 0.25 or 0.5 g 30:70 ACN/DI water, depending on the volume of the introduced IS, for quantitation using LC-MS/MS detection.

Shrimp and fish tissues. A general homogenization technique was used to extract subsamples from whole shrimp and fish tissue – brain, kidney, liver and white muscle – for IMI residue quantification. Whole shrimp (5.0 – 12.0 g) were transferred from storage at -80 °C to -20 °C

the day before processing. Fish tissues (0.3 – 10.0 g) were removed from storage at -80 °C the day of processing and allowed to thaw to room temperature. Frozen shrimp and thawed fish tissues were placed on a Teflon cutting board. Shrimp were minced with a butcher's knife, fish tissues with a #20 scalpel, transferred to 50-mL conical tubes and mass recorded. A roughly equivalent mass of DI water was added for an approximately 2x sample dilution. The samples were homogenized with a rotor/stator type tissue homogenizer (Tissue Tearor™ Model 398, Biospec Products) set at maximum power for 2 -3 min. Subsamples of homogenate (0.2 – 0.3 g) were transferred to 50.0 mL conical tubes and 0.025 g 1000 μg L^{-1} IS introduced. IS equilibration, tissue disintegration via sonic dismembration, and extraction / drying of supernatant was as described for plasma and bile. Dried samples were reconstituted in 3 mL DI water and vortexed vigorously for 1 min. The aqueous samples were transferred to SPE columns for reversed phase SPE as described for sediment pore water. After drying, the samples were reconstituted in 0.5 g 30:70 ACN/DI water for quantitation using LC-MS/MS detection.

(c). ELISA screening protocol

Plasma aliquots (0.5 g) were transferred to 50-mL conical tubes and 5 mL ACN and 250 mg NaCl were added. The samples were placed on ice and homogenized using a sonic dismembrator (Model 4C15, Fisher Scientific) set at maximum power for 2 min., followed by vigorous vortexing for 1 min. The supernatant was collected from each sample following centrifugation at 4000 x *g* for 15 min., transferred to a glass evaporation tube, and dried under N_2 in a vacuum manifold. Dried samples were reconstituted in 3.0 g DI water, followed by reversed phase SPE, as described previously. Samples were reconstituted in 10.0 g DI water for quantitation using ELISA detection (Quantiplate Kit for Imidacloprid, EnviroLogix), following the manufacturer's protocol [38].

2. Toxicity of derivatives

As previously discussed, IMI is a neurotoxicant that acts as an agonist at acetylcholine (ACh) binding sites on nicotinic acetylcholine receptors (nAChRs). The electronegative nitroguanidine moiety on IMI has been identified as the pharmacophore, responsible for the selective binding to invertebrate versus vertebrate nAChRs [16, 39-42]. H-bonding between this functional group and specific invertebrate cationic amino acid residues, or repulsion by anionic residues in vertebrates, accounts for this selectivity (Fig. 3) [16, 42].

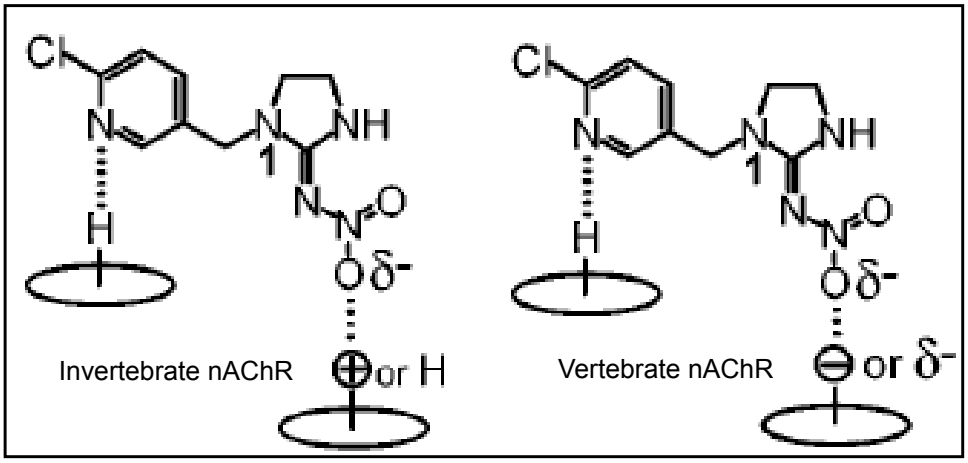

Fig. 3. Selective binding affinity of IMI to invertebrate nAChR (Tomizawa et al., 2000).

Derivatives with structural changes at the pharmacophore may possess equivalent or greater binding affinity for vertebrate nAChRs compared with the parent compound [43]. A preliminary screening was made of compounds possessing pharmacophore modifications through a literature review of hydrolytic, photolytic, plant, and soil degradation pathways [18, 44-46].

Following preliminary identification, further literature research was conducted on the potential toxicity of these candidate derivatives. No toxicological studies on any of the identified derivatives were available for review. In lieu of definitive exposure studies *in vivo*, a literature

review was conducted to find evidence of the potential toxicity of these metabolites based on findings from *in vitro* studies. Results from competitive binding assays were used for determining the binding potency of the derivatives relative to the parent compound. This approach measures the ability of the compound of interest to displace a radioligand (e.g., [^{3}H]IMI) from its binding site on vertebrate α4β2 nAChR subtype membrane preparations. The IC_{50} is the concentration of the compound resulting in 50% displacement of the radioligand, and is inversely related to its potency (i.e., lower value indicates greater potency) [47, 48]. Inferences on the potential toxicity of the derivatives to green sturgeon were made based on the findings from these studies along with the relative bioavailability of the compounds.

3. Confirmation of opportunistic feeding

(a). Test beds

IMI was applied to four test plots totaling 6.4 ha (15.8 ac) on tidal mudflats north of Nahcotta, WA in Willapa Bay using the proposed operational formulated product (Nuprid® 2F, 21.4% active ingredient (a.i.), Nufarm Americas, Inc.) at an application rate of 0.56 kg ha^{-1} a.i. Bed boundaries and sampling locations were defined using a global positioning system (GPS) transceiver (Garmin GPSmap 60Csx, Garmin Ltd.). The beds were designated treatment beds north (TB-N), central (TB-C) and south (TB-S). These were aligned along a north-south axis spaced approximately 200 m apart. Areas for each, from north to south were 0.9 (2.3), 1.9 (4.8), and 1.2 (2.9) ha (ac), respectively. A 2.0 ha (5.0 ac) "L" shaped control bed (CB) was located approximately 200 m north of the northern-most treatment bed (Fig. 4).

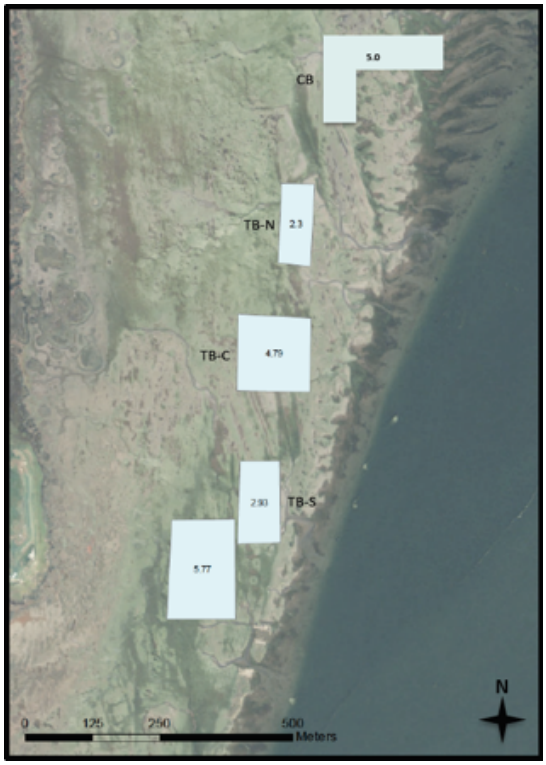

Fig. 4. IMI treatment beds (TB-N, -C, -S) and control bed (CB) on Willapa Bay north of Nahcotta, WA (the southernmost treatment bed was not used due to restrictions on accessibility).

(b). Sample and pit count locations

Sediment and shrimp sampling locations were designated on each bed. TB-N and TB-S were subdivided into three equivalently sized subplots numbered 1-3 along the north-south axis (Fig. 5A). TB-C was subdivided into six equivalently sized subplots in a 2x3 grid (Fig. 5B). Six subplots were also designated on CB: four along the east-west axis and two adjoining south of the northwest subplot (Fig 5C). Stakes marked the sampling locations at the center of each subplot. Reference points for sturgeon pit counts were established by placing stakes at two randomly selected locations approximately 15 m north, south, east or west (N, S, E, W) from each sampling location (Fig. 5A-C).

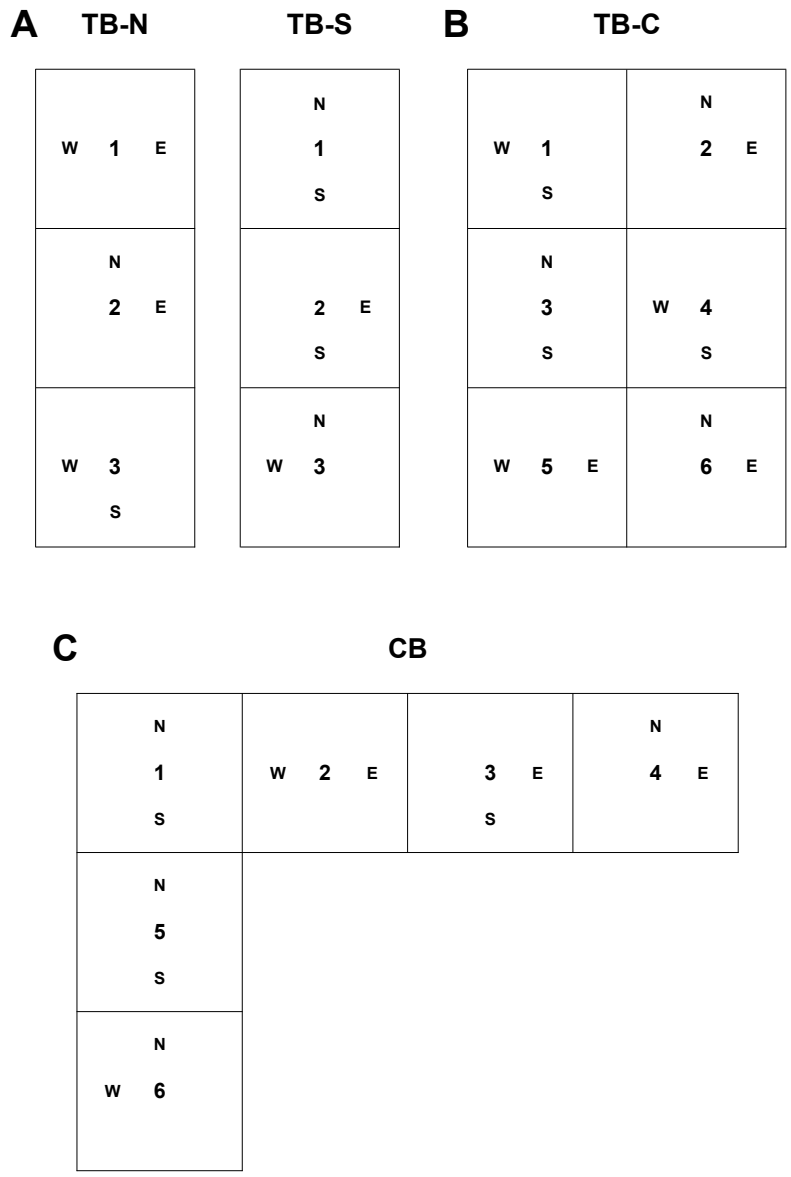

Fig. 5. Subplot and sampling designations for treatment and control beds. (**A**) North and south treatment beds (TB-N, TB-S). (**B**) Central treatment bed (TB-C). (**C**) Control bed (CB).

Sturgeon pits were counted around each defined reference point at low tide. Recordings were made within a 50 m^2 area while walking along the circumference of a circle defined by the endpoint of a 4 m rope attached to each sturgeon pit reference stake. All pits that were one-half or more inside the defined area were counted. Normal feeding activity was monitored by counting sturgeon pits on the control (n = 12) and treatment (n = 24) beds 24 h preceding

chemical treatment and on the day of application (IMI application and pit counts were made at the morning low tide, prior to potential sturgeon predation following the incoming high tide). Post-application pit counts were made at 24, 48, 72 and 96 h on the control and treatment beds.

4. Exposure characterization

Clam guns (63.5 cm long, 10.1 cm wide) were used for excavating cores for the collection of sediment and shrimp. Each coring device was used once per sampling location each day. The coring devices were decontaminated prior to use the following sampling day. All samples were taken at low tide. Following removal of the core, any water collected above the surface of the sediment was decanted. Shrimp were collected from the cavity of the removed sediment and within the core. Recordings were made of the condition (alive or dead) and gender of the shrimp. Females were listed as gravid or non-gravid. The shrimp were then placed individually in plastic bags, and stored on ice in a closed cooler at a temperature of 2-4 °C. Only *N. californiensis* were collected. The accompanying sediment core was deposited into a 19 L plastic bucket. The bucket was covered with a disposable plastic liner that was replaced after each collection. The sediment was mixed by hand thoroughly for approximately 2-3 min. An approximately 1500 g subsample of the homogenate was transferred to a 1-L Nalgene® HDPE container and immediately stored on ice in a closed cooler at a temperature of 2-4 °C to prevent photolytic degradation [45]. Upon completion of the daily field collections, shrimp samples were transferred to a freezer and stored at -20 °C. Following transport to the UW in closed coolers on dry ice, shrimp were stored at -80 °C until IMI residue quantification. The sediment samples were transferred to a refrigerator and stored in darkness at 4 °C. Samples were transported to the UW on ice in closed coolers at 2-4 °C for pore water extraction and IMI

residue quantification within the prescribed 7-d holding period (previous studies revealed that the hydrolytic ½-life, when measured at 25 °C and pH 7, was greater than 30 days [49, 50]).

Sediment samples were collected for analysis at one randomly chosen sampling site on the control, north and south treatment beds, and two locations on the central treatment bed, 24 h prior to IMI application for verification that the beds were clean. Likewise, sediment samples were taken at two randomly chosen sites on the control bed 24 h post-IMI application for determination of potential IMI carry-over contamination from the treatment beds. Sediment samples were collected at randomly selected locations on the north and south treatment beds (n = 1 each) and central treatment bed (n = 2) within 1 h post-application of IMI. Sediment and shrimp samples (n = 12 ea) were collected from all sites on the treatment beds at 24, 48, 72 and 96 h post IMI application.

Two additional core samples (diameter and depth = 7 and 10 cm, respectively), obtained using the same extraction method described below in section 7(b) of the Methods section, were taken from the center sampling locations prior to IMI application on the north and south treatment beds – TB-N-2 and TB-S-2 – for sediment characterization by a contract laboratory (Analytical Resources, Inc.).

5. *Exposure verification*

Green sturgeon sampling was conducted in collaboration with the Washington Department of Fish and Wildlife (WDFW) as part of their annual monitoring program under guidelines set by the National Marine Fisheries Service (NMFS) [1]. A chartered commercial fishing vessel was used for capturing fish by long-line gill netting at multiple locations in proximity to IMI test beds during high tide. Green sturgeon (n = 20 per day) were captured approximately 18 h pre- and 30

h post-application of IMI. Following capture, 5–10 mL of blood – depending on the size of the fish – was withdrawn from the caudal vein by needle attached to a 5- or 10-mL heparinized vacuum reservoir (BD Vacutainer, Becton Dickinson). The withdrawn blood was placed on ice in a closed cooler for 2-4 h. Upon returning to shore, plasma was isolated (3000 x *g*, 10 min.) and 2-mL aliquots from each fish were stored on dry ice in a closed cooler. Following transfer to the UW, the plasma was stored at -80 °C until IMI residue quantitation.

6. Uptake estimation

(a). Branchial uptake

An established flow-limited model for chemical uptake across fish gills was used to estimate branchial uptake of IMI in green sturgeon [51]. This model calculates branchial flux (i.e., the rate of chemical transfer across the membrane) from potential rate limitations imposed by the capacity of inspired water to deliver chemical to the gills, along with the capacity of blood to remove chemical from the gills, assuming no diffusion limitations. Given these factors, an empirical relationship was developed for predicting branchial uptake in RBT based on the chemical log K_{ow}. The prediction of branchial uptake of IMI in green sturgeon assumed that any morphological differences between RBT and green sturgeon, such as gill geometry, the weight-normalized respiratory volume, and cardiac output had no bearing on this relationship.

(b). Dietary uptake

A model based on assimilation efficiency (AE) – the fraction of chemical absorbed from the total amount ingested by the fish – was initially selected for use in predicting dietary uptake. This model was based on results from a literature review of the measured uptake efficiency of multiple chemicals in food consumed by several species of fish [52].

7. White sturgeon controlled exposure studies

The Spokane Indian Tribe provided two cohorts of juvenile hatchery-reared freshwater (FW) white sturgeon. These fish were raised at the WDFW Columbia Basin Hatchery in Moses Lake, WA as part of the Lake Roosevelt White Sturgeon Recovery Project [53].

(a). Sturgeon sensitivity to IMI

An initial cohort of young-of-the-year (YOY) white sturgeon was transported to the UW. Fish were maintained for approximately 1 month in flowing de-chlorinated City of Seattle water at an approximate photoperiod of 16D/8N. Temperature (14.0 ± 1.0 °C), dissolved oxygen (D.O. – 10.0 ± 1.0 mg L^{-1}) and pH (7.1-7.4) were monitored daily. The average mass of the fish was calculated. Fish were fed BioDiet Grower, 3.0 mm (Bio-Oregon) twice daily at a combined rate of 2.5% body weight.

A 96-h median lethal toxicity (LC_{50}) test was conducted under USEPA acute toxicity test procedures and in accordance with guidelines set by the UW Institutional Animal Care and Use Committee (IUCAC) under Protocol Number 2185-30 [54]. Juvenile white sturgeon were fasted 48 h prior to the beginning of the test. The test was conducted using filtered City of Seattle FW in a temperature-controlled environmental chamber in 210-L vessels with food-grade clear plastic liners under static conditions with supplemental aeration. Five fish were placed into each vessel. The average mass of the fish was 27.7 g. Loading of fish did not exceed 0.8 g fish weight per L test solution. The approximate photoperiod was 16D/8N. Test concentrations of IMI were generated using the Nufarm 2F formulated product in a 1.45 geometric progression of 46, 66, 96, 139 and 202 mg L^{-1}, with one tank per concentration plus control. This concentration series approximated the one used in a previous 96-h median lethal toxicity test with SW-adapted juvenile Chinook (*Oncorhynchus tshawytscha*), with a resulting LC_{50} of 109 mg L^{-1} [55]. Use of

this geometric series was based on the assumption that white sturgeon would exhibit similar sensitivity to IMI as juvenile Chinook. Temperature, DO, pH and conductivity (adjusted to specific conductance @ 25 °C) were monitored following test initiation and at 6, 24, 48, 72 and 96 h thereafter. Temperature was held at 14.0 ± 1.0 °C, D.O. at 10.0 ± 1.0 mg L^{-1} and pH at 7.1-7.4. Specific conductance ranged from 56 µs cm^{-1} in the clean water control to 89 µs cm^{-1} in the highest test concentration. Observations of the physical condition of individual fish were recorded at the same time periods. Fish were euthanized at test completion.

(b). IMI field exposures and plasma residue concentrations

Additional exposures with white sturgeon were based on field data collected and analyzed following application of the Nufarm® 2F formulated product at a rate of 2.24 kg a.i. ha^{-1} (2.0 lb. a.i. ac^{-1}) on test beds in Willapa Bay in July 2010. At the time of the 2010 test applications, the WGHOGA planned to seek a registration for the 2.24 kg a.i. ha^{-1} application rate. The association later reduced this to 0.56 kg a.i. ha^{-1} – the application rate that was used on the test beds in July 2012 as described in the present exposure characterization.

Exposure scenario. A "worst-case" exposure scenario was modeled based on measurements of IMI in pore water samples that were collected from three sampling locations on a test bed in Willapa Bay in July 2010 at 0, 12 and 24 h following application of the Nufarm® 2F formulated product at a rate of 2.24 kg a.i. ha^{-1}. A semi-transparent 500 mL bottle (Nalgene® Narrow-Mouth Bottle, PP, Nalge Nunc Int'l.), with the bottom removed and vent hole on the top shoulder, was used for collecting a sediment sample 7 cm in diameter and 10 cm in depth. A clean coring device was used at each sampling location/time interval. Any surface water collected above the sediment was decanted following removal of the core. Two cores were collected at each sampling location. Both cores were placed in a 1 L Nalgene® HDPP container

with a combined mass of approximately 1500 g, and immediately stored on ice in a closed cooler at a temperature of 2-4 °C. The samples were transferred to a refrigerator and stored in darkness at 4 °C following field collection. Samples were transported to the UW on ice in closed coolers at 2-4 °C for pore water extraction within the prescribed 7-d holding period, as described previously. The extracted pore water was shipped overnight in clean 125 mL amber glass bottles on ice at 2-4 °C to a contract analytical chemistry laboratory (Pacific Agricultural Laboratory – PAL – Portland, OR). Reported average concentrations at 0, 12 and 24 h post-application were 1227, 537, and 27 μg L^{-1}, respectively. An exponential equation was fitted to the data points using Excel (Microsoft Corp.) for estimation of pore water concentrations at 6, 18 and 30 h – the approximate peak high tide times over three successive tidal cycles – following IMI application (Fig. 6). Estimated pore water concentrations were 678, 100 and 15 μg L^{-1} at 6, 18 and 30 h, respectively. The decrease in chemical concentration at successive high tides approximated the tidal "flushing" of the beds (this rapid loss of chemical from the beds in consecutive tidal cycles was also observed in the 2012 sampling effort following the 0.56 kg a.i. ha^{-1} application rate described below in the exposure characterization section). These concentrations were subsequently used in the worst-case white sturgeon exposures. Concentration estimations were also made at these time points for an IMI application at a rate of 0.56 kg a.i. ha^{-1} – ¼ the amount initially proposed by the oyster growers. This was achieved by dividing the measured pore water concentrations at the 2.0 a.i. per acre application by four and fitting an exponential equation to the data points using Excel. The latter concentrations following the regression analysis at $1/4^{th}$ the measured values at 0, 12 and 24 h post-IMI application were 169, 25 and 4 μg L^{-1} at 6, 18 and 30 h, respectively.

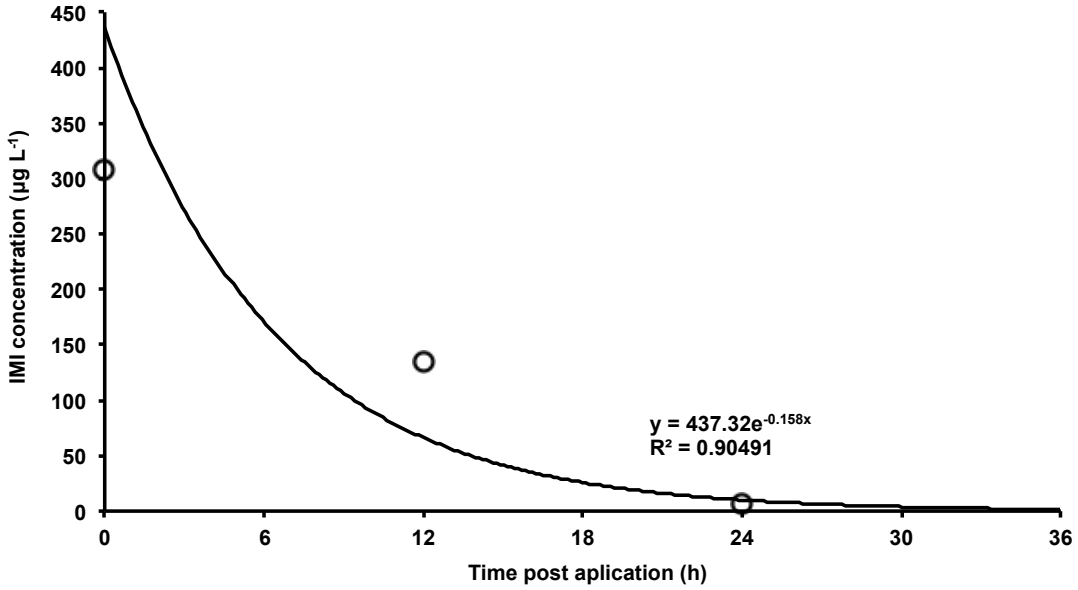

Fig. 6. 2010 Willapa Bay pore water IMI residue concentration regression analysis based on measurements at 0, 12 and 24 h post-application.

SW acclimation. A second cohort of YOY white sturgeon was transported from the Columbia Basin Hatchery to the UW for controlled IMI exposures in seawater (SW) at concentrations and durations simulating expected worst-case scenarios in the field. Due to size and age constraints, these fish were not capable of successfully acclimating to SW upon receipt from the hatchery [56]. The fish were therefore maintained at the UW for 1 year to ensure adequate size and maturity for SW acclimation. The fish were housed in circular tanks with flowing de-chlorinated City of Seattle water. Temperature (14.0 ± 1.0 °C), dissolved oxygen (D.O. (10.0 ± 1.0 mg L^{-1}) and pH (7.1-7.4) were monitored daily. The average mass of the fish was calculated on a monthly basis, and the fish were fed BioBrood, 4.0 mm (Bio-Oregon) once daily at rates relative to percent body weight, decreasing as they grew in size from 1.95 to 0.95% over approximately 6 months. The fish were then fed BioBrood 6.0 mm at a once-daily rate of 0.95% body weight.

Upon achieving adequate age and size, the fish were transferred to the USGS Western Fisheries Science Center, Marrowstone Marine Station in Norland, WA and SW acclimated in a large circular tank with an adjustable mixture of flowing sand-filtered SW at 30 parts per thousand (ppt) salt concentration and flowing de-chlorinated FW from the City of Port Townsend, WA. SW acclimation was accomplished as follows: the fish were held for 2 days at an isotonic concentration of 8 ppt, then 5 ppt increases every 2 days (8, 13, 18, 23 and 28 ppt) followed by a final 2 ppt increase to full SW (30 ppt). The fish were maintained in the tank with flowing SW and supplemental aeration for approximately 2 months prior to the controlled IMI exposures. Temperature (10.0 ± 1.0 °C), D.O. (9.02 – 10.15 mg L^{-1}), pH (10.0 ± 1.0) and salinity (30.0 ± 1.0) were monitored daily. The average body mass was calculated monthly, and the fish were fed BioBrood 6.0 mm at a once-daily rate of 0.95% body weight.

Exposure tests. Test concentrations of IMI for the exposures were generated using the Nufarm 2F formulated product. Due to difficulty in calculating and administering dietary contributions, water was the only route of IMI exposure (it was later determined that branchial uptake of IMI was far greater than dietary uptake). It was assumed that green sturgeon would be exposed to IMI – present in the sediment pore water – at the concentrations determined as discussed above, while digging for burrowing shrimp for the entire duration of three successive 6-h high-tide cycles (i.e., at 6, 18 and 30 h post-application).

Test fish were removed from the large holding tank and placed into one of four circular exposure tanks. Given the truncated 6-h exposure time and relatively large size of the test animals, an adjusted loading of 0.05 g fish weight per L solution was adhered to for compliance with USEPA standard 96-h acute static exposure guidelines [54]. Exposure tests were conducted at both the 2.24 kg a.i. $ha^{-1}$and the 0.56 kg a.i. ha^{-1} application rates. Fish (n = 24 per test) were

exposed to one, two, or three successive high tide concentrations for 6 h under static conditions with supplemental aeration. At the end of each exposure period, a subset of fish (n = 8) was removed for extraction of blood and livers. The remaining fish were transferred to tanks with clean flowing SW for a 6-h recovery period, simulating movement off of the beds during low tide. Temperature, DO, pH and salinity were measured at the beginning and end of each exposure and recovery period. Temperature was held at 12.0 ± 1.0 °C, D.O. at 10.0 ± 1.0 mg L^{-1}, pH at 6.4-6.8, and salinity at 30.0 ± 1.0 mg L^{-1}.

Fish were removed from the exposure tank and stunned by administering a blow to the head. Length and weight measurements were recorded. First gill arches were severed and blood collected using pre-heparinized 5-mL syringes. Blood was transferred to 15 mL conical tubes and centrifuged for isolation of plasma (1900 x *g*, 10 min.). Plasma was transferred to 1.5 mL centrifuge tubes and stored at -80 °C. Livers were excised with gall bladders intact, transferred to 50-mL conical tubes and stored at -80 °C. The remaining carcasses were stored at -40 °C. All samples were transferred to the UW in closed coolers on dry ice.

(c). Persistence of IMI in sturgeon

Test fish were transferred to the exposure tanks as discussed above. Fish (n = 28, plus 4 controls, 1.3-1.6 kg) were exposed to IMI at the first concentration from the 2.24 kg a.i. ha^{-1} simulated field exposure (678 μg L^{-1}) for 6 h under static conditions with supplemental aeration. Loading of fish did not exceed 0.05 g fish weight per L test solution. Temperature, D.O., pH and salinity were measured at the beginning and end of the exposure and recovery periods. Temperature was held at 12.0 ± 1.0 °C, D.O. at 9.0 ± 1.0 mg L^{-1}, pH at 6.8-7.0, and salinity at 30.0 ± 1.0 mg L^{-1}. Following exposure, the fish were transferred to clean SW. Four fish were

removed for processing and storage as described above at time intervals 0, 1, 2, 4, 8, 16 and 32 h following the end of the exposure.

8. Rainbow trout toxicokinetics studies

Toxicokinetic studies with RBT were conducted at the USEPA Mid-Continent Ecology Laboratory in Duluth, MN. Juvenile RBT were obtained from the USGS Upper Midwest Environmental Sciences Center in La Crosse, WI. Fish husbandry was in accordance with USEPA standard operating procedure (SOP) CULT-002 published 24 October 1997 and revised 28 November 2007. Fish were raised to the necessary size for each experiment. All were maintained in sand-filtered Lake Superior water on a natural photoperiod and fed Nelson's Silver Cup Trout Feed (Nelson and Sons, Inc.). Water quality characteristics were measured and recorded daily. Temperature was held at 11 ± 1 °C, D.O. at 85-100% saturation, pH at 7.6-7.8, total ammonia at < 1 mg L^{-1}, water hardness (as $CaCO_3$) at 45-46 mg L^{-1}, and alkalinity at 41-44 mg L^{-1}. All tests were in accordance with guidelines set by the USEPA Mid-Continent Ecology Division Animal Care and Use Committee (ACUC). IMI concentrations were prepared using the same IMI reference standard identified previously.

Preliminary depuration study. An initial study was conducted with the goal of gaining insight into the disposition of IMI in RBT following bolus inter-arterial injection of a nominal dose. The dose was determined based on observations from the juvenile Chinook IMI acute toxicity test described previously. Residue concentrations in brain tissue from these fish approximated the water concentrations following 96-h IMI exposures [55]. The no observed adverse effect concentration (NOAEC) subsequent to these exposures was approximately 40 mg L^{-1}. A 20-fold safety factor was placed on the approximated maximum asymptomatic IMI tissue

concentration of 40 mg kg^{-1} in juvenile Chinook for a nominal dose value of 200 µg kg^{-1}. Distribution of IMI throughout the body was assumed to be instantaneous following administration of the dose. Information gained from this investigation was used for determining the critical inputs of dose, sampling intervals and test duration for the second study – all of which were essential for deriving the primary TK parameters.

The elimination of IMI from plasma was measured in fourteen fish (94-259 g). Fish were anesthetized with 300 mg/L tricaine methanesulphonate (MS-222) buffered with 900 mg L^{-1} $NaHCO_3$. The IMI dosing solution was prepared using Cortland's physiological saline [57]. The dose was administered to each fish through the dorsal aorta at a volume of 100 µL per 100 g fish mass. After injection, each fish was placed in an individual tank with clean flowing water from the same source used for husbandry. Recovery/depuration times were 1, 4, 10 and 24 h, with n = 4, 4, 3, 3 fish per time period, respectively.

Each fish was anesthetized in MS-222 following removal from the recovery tank and euthanized via exsanguination. Blood was withdrawn from the caudal vein using a pre-heparinized, 2-mL syringe and transferred to a 1.5-mL centrifuge tube. Blood was centrifuged at 5000 x *g* for 10 min to obtain plasma. The plasma was transferred to a clean 1.5-mL centrifuge tube, flash-frozen in liquid N_2 and stored at -80 °C. Liver, kidney and white muscle were removed and the mass of each recorded. Samples were flash-frozen in liquid N_2 and stored along with the bodies at -80 °C. All samples were shipped overnight to the UW on dry ice and stored at -80 °C until IMI residue analysis.

Definitive depuration study. A second set of injection experiments was conducted following analysis of the IMI residue data from the preliminary depuration study. The goals of this study were to develop plasma concentration-time profiles for determination of the elimination rate

constant for the terminal phase (k); derive the terminal phase half-life ($t_{½}$) and the principal TK parameters CL, V, and AUC; assess the potential contribution of branchial elimination to overall loss of the chemical; examine the distribution of the compound by calculating a set of plasma-tissue concentration ratios; and assess the potential for dose-dependent kinetics at two environmentally relevant chemical concentrations.

The injection experiments were conducted with fish that were surgically prepared for containment and restraint in individual chambers, as described previously [58]. Briefly, fish were anesthetized with MS-222. A spinal transection was performed to immobilize each fish, and a cannula was inserted into the dorsal aorta. A urine catheter was inserted successfully in one of the fish. A latex oral membrane was fitted and sewn over the mouth of each fish to permit separate collection of inspired and expired water.

Following surgery, the fish was placed into a compartmentalized acrylic plastic chamber (Fig. 7). Acrylic plastic barriers separated the three compartments, Chambers A-C. The oral membrane sewn on the fish was attached to a support at the opening between the inflow compartment (Chamber A) and the expired water compartment (Chamber B). Water from Chamber A could only move to Chamber B through respiration of the fish. D.O. was monitored in the inflowing water. Excess water not inspired by the fish flowed out of Chamber A through an adjustable standpipe. A latex membrane covered the opening between Chambers B and C. This membrane was fitted over the body of the fish immediately posterior to the gills, preventing passage of expired water into Chamber C. Water flowed out of Chamber B through an adjustable standpipe. A meter connected to the outflow tube of the standpipe monitored flow rate across the gills. The latter part of the body within Chamber C was held in place by supports. The ventilation volume of each fish was monitored following placement in the chambers using

an automated data collection system utilizing customized software [59]. Water quality parameters (D.O., pH, and temp.) were also monitored.

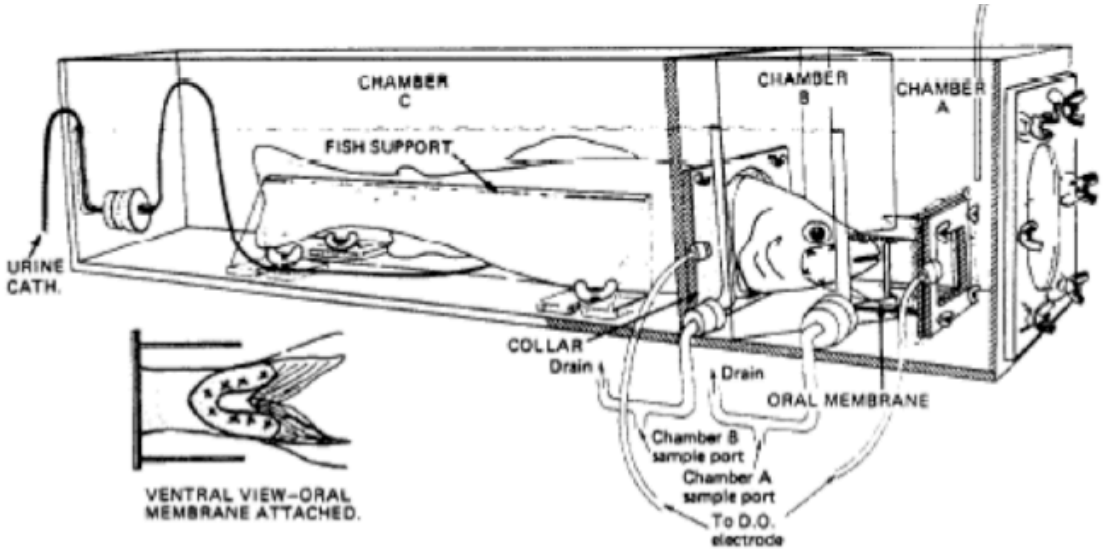

Fig. 7. Chamber used for second toxicokinetics study (illustration courtesy of [58]).

Two groups of fish received different doses. Five fish (843-1050 g) were injected with a 250 μg kg^{-1} b.w. IMI "high" dose, while another five fish (704-1245 g) received a 25 μg kg^{-1} "low" dose. Bolus injections (100 μL per 100 g body weight) were administered through the dorsal aortic cannula.

Replicate blood samples (50 or 100 μL) were collected at pre- and 1, 2, 4, 8, 16, 24, 36 and 48 h post-injection. Blood samples were withdrawn from the dorsal aortic cannula with pre-heparinzed capillary tubes. Following termination of the experiment at 48 h, 3-5 mL of blood were withdrawn from the caudal vein and transferred to 1.5 mL microcentrifuge tubes. Blood was centrifuged at 5000 x *g* for 10 min to obtain plasma. The plasma was transferred to clean 200 μL picocentrifuge or 1.5 mL microcentrifuge tubes, flash-frozen in liquid N_2 and stored at -

80 °C. The samples were shipped overnight to the UW on dry ice and stored at -80 °C until IMI residue analysis.

Approximately 250 mL of branchial water (i.e., water expired across the gills) was collected from the outflow tube of Chamber B in Nalgene bottles concurrent with blood at each time interval. Low and high dose samples at time intervals 1-8 h were stored temporarily at 4 °C prior to IMI residue concentration utilizing reverse-phase SPE as discussed previously. The remaining samples were frozen at -80 °C before shipment overnight to the UW on dry ice. Samples were then stored at -80 °C until IMI residue concentration and quantitation.

Brain, kidney, liver, white muscle and bile were removed and masses recorded. Samples were flash-frozen in liquid N_2 and stored at -80 °C. All samples were shipped overnight to the UW on dry ice and stored at -80 °C until IMI residue analysis.

9. Hepatic metabolism.

Active and heat-denatured RBT liver S9 subcellular fractions were prepared following an established protocol [60, 61]. The reaction mixtures (200 µL total volume) consisted of S9 protein (1.0 mg mL^{-1}), β-NADPH (2.0 mM), UDPGA (2.0 mM), GSH (5.0 mM), adenosine 3'-phosphate 5-phosphosulfate – PAPS (0.1 mM), and alamethicin (25.0 µg mL^{-1} in 100 mM potassium phosphate buffer, pH 7.8).

Three sets of solutions were prepared: matrix blank solutions containing active S9, alamethicin and cofactors without substrate; active solutions containing active S9, alamethicin and cofactors with substrate; and control solutions containing heat-denatured S9, alamethicin and cofactors with substrate [61].

Aliquots of 2.0 or 20.0 μM IMI substrate prepared in KPO_4 buffer (100 mM, pH 7.8) were added to the prepared S9 solutions for final reaction concentrations of 0.1 and 1.0 μM IMI, respectively. Active and denatured samples were run in duplicate at an incubation schedule of 0, 20, 40, 60, 120, 150 and 180 min. Following the addition of substrate, the test solutions were incubated at 11 °C in a covered shaker water bath. Reactions were terminated by the addition of 600 μL of ice-cold ACN. Samples were stored at 4 °C prior to being shipped overnight to the UW on dry ice and stored at -80 °C until IMI residue analysis.

RESULTS AND DISCUSSION

1. Detection protocol and sample preparation optimization.

Nominal responses between the 1.0, 10.0, 100.0 and 1000.0 μg L^{-1} IMI and 50 μg L^{-1} IS standards were 0.02, 0.2, 2.0 and 20.0, respectively. Coefficients of determination (R^2) for the fitted curves were ≥ 0.9999. A limit of quantification (LOQ) of 1.0 μg L^{-1} was confirmed on all LC-MS/MS runs. A signal-noise ratio of 10:1 or greater was measured between the area (m/z ratio) of the lowest calibrated standard, 1.0 μg L^{-1}, and the matrix background. A 0.3 μg L^{-1} limit of detection (LOD) was determined based on a 3:1 signal-noise ratio. Carry-over – calculated by measuring the difference between the IMI/IS ratios of the highest calibration standard (1000.0 μg L^{-1}) and a succeeding "blank" run consisting of LC solvents only – was consistently measured between 0.05 – 0.1%.

Validation studies were conducted for determination of the variability in IMI residue values quantitated in samples following LC-MS/MS detection. Variances within and between LC-

MS/MS runs (i.e., intra- and inter-assay variability, respectively), and differences between sample preparations (i.e., technical replication) were determined.

Inter-assay variability and technical replication. Plasma samples were obtained from three high-dose RBT in the definitive depuration study at 48 h post-injection of IMI (H1-48, H2-48 and H4-48). Three sample preparations, labeled A-C, were made from each of the plasma samples. IMI residues from all nine of these subsamples were quantitated using LC-MS/MS detection on three successive days (Table 1).

Table 1. Plasma IMI residue concentrations calculated following three LC-MS/MS analyses.

	Concentration (μg kg^{-1})			
Subsample	Analysis 1	Analysis 2	Analysis 3	Avg.
H1-48-A	74.5	78.3	72.5	75.1
H1-48-B	80.8	82.7	78.0	80.5
H1-48-C	78.4	79.0	77.4	78.2
H2-48-A	89.0	89.5	89.3	89.3
H2-48-B	88.8	88.3	87.2	88.1
H2-48-C	84.5	90.5	88.3	87.8
H4-48-A	68.3	66.6	66.9	67.2
H4-48-B	69.5	69.6	68.1	69.1
H4-48-C	69.5	68.4	70.6	69.5

Quantitated values for each subsample (n = 9) were compared across the three detection days for measurement of inter-assay variability. The relative standard deviation (RSD) for the subsamples ranged from 0.2 to 3.9% (Table 2).

Table 2. Inter-assay variability among subsamples of plasma.

Subsample (n = 3/ea)	RSD (%)
H1-48-A	3.9
H1-48-B	2.9
H1-48-C	1.0
H2-48-A	0.2
H2-48-B	0.9
H2-48-C	3.5
H4-48-A	1.3
H4-48-B	1.2
H4-48-C	1.5

Technical replication was measured by comparing the variation in calculated concentrations among subsamples for each plasma sample on all three LC-MS/MS analysis days. The RSD for the subsamples ranged from 1.0 to 4.1% (Table 3).

Table 3. Technical replication among subsamples following three LC-MS/MS analyses.

	RSD (%)		
Subsamples	Day 1	Day 2	Day 3
H1-48-(A-C)	4.1	3.0	3.9
H2-48-(A-C)	2.9	1.2	1.2
H4-48-(A-C)	1.0	2.2	2.7

Technical replication was also measured for the more complex tissue/shrimp sample preparation. Three subsamples were processed from a homogenized shrimp collected from the field 24-h post-IMI application. The RSD following quantitation was 4.8%.

Intra-assay variability. Three measurements were made for sample preparations H1-48-(A-C) on the first LC-MS/MS run (Table 4).

Table 4. Plasma IMI residue concentrations calculated in H1-48 subsamples following LC-MS/MS analysis.

Subsample	Concentration (μg kg^{-1})
H1-48-A1	74.5
H1-48-A2	74.0
H1-48-A3	75.7
H1-48-B1	80.8
H1-48-B2	79.5
H1-48-B3	78.6
H1-48-C1	78.4
H1-48-C2	76.0
H1-48-C3	78.4

Intra-assay variability was determined for the three sample preparations made from plasma sample H1-48 by comparing the three calculated IMI residue concentrations for each subsample. The RSD for the subsamples ranged from 1.2 to 1.8% (Table 5).

Table 5. Intra-assay variability among H1-48 subsamples.

Subsample (n = 3/ea)	RSD (%)
H1-48-A	1.2
H1-48-B	1.4
H1-48-C	1.8

The methods validation, through adherence to quality control procedures, demonstrated that the sample preparation protocols and LC-MS/MS method would consistently generate appropriate data [37]. Variations in results presented below were expected to fall within the boundaries identified in the validation study.

ELISA protocol validation. The LOQ and LOD, as stated by the manufacturer, were 0.2 and 0.07 μg L^{-1}, respectively. Reconstitution of the samples resulted in a 20x increase in these limits to 4.0 and 1.4 μg L^{-1}. The average background-blanked absorbance (BBA) from measured clean

plasma samples (n = 6) relative to the ELISA negative control was 85.2 % (standard deviation – SD = 2.5%). The average background concentration was 1.8 μg kg^{-1} (SD = 0.1 μg kg^{-1}). Two plasma samples spiked with IMI at a nominal concentration of 40.0 μg kg^{-1} had recoveries of 81 and 74%.

Measurements made with the ELISA do not differentiate between the detected concentration of IMI and specific metabolites [38, 55]. The relative complexity of the sample preparation limited the effectiveness of the approach for its intended purpose as a high-throughput screening tool for environmental monitoring. Due to this limitation, use of the ELISA was discontinued. ELISA detection was used for quantitation of a subset of white sturgeon plasma samples following controlled IMI exposure as discussed below, however (these samples were the first to be analyzed, prior to adoption of LC-MS/MS detection).

2. Toxicity of derivatives

Two derivatives, IMI-guanidine and IMI-guanidine-olefin, were found to have IC_{50} values for the vertebrate α4β2 nAChR preparations that were considerably lower than the parent compound (no measurements were identified in the literature review pertaining to the relative contribution of these metabolites to the overall quantity of IMI break-down products). IC_{50} values vary across assays, and cannot be used as a direct indicator of binding affinity. Despite this limitation, the toxicity of both derivatives was estimated based on their relative potency, measured as the ratio of the IC_{50} value of the parent compound and the derivative in each assay. The relative potency of each derivative was greater than IMI (Table 6).

Table 6. Calculated median inhibitory concentration (IC_{50}) values and potency increases for IMI, IMI-guanidine and IMI-guanidine-olefin to mouse nAChR preparations (adapted from [31]).

	Mouse (*Mus musculus*) α4β2 IC_{50} (nM)	Relative potency
IMI	2600	N/A
IMI-guanidine	8.2	317
IMI-guanidine-olefin	23	113

Because the toxicity of these compounds is greatly influenced by their bioavailability (i.e., the extent to which the chemicals in the exposure environment are accumulated in the organism of interest), relative toxicity *in vivo* cannot be determined by a simple extrapolation of the target site potency. As suggested by their names, the IMI-guanidine and IMI-guanidine-olefin derivatives share an identical pharmacophore modification: an electro-positive guanidine. The guanidine moiety on has a $pK_a > 12$ [62]. A positively charged resonance structure predominates at environmental and physiological pH [42]. This can be illustrated by use of the Henderson-Hasselbach equation: assuming an environmental and physiological pH of 7.4 and a guanidine pK_a of 12, the ionized / un-ionized species ratio for the guanidine derivatives would be approximately 1.0×10^5 [63].

Passive diffusion across epithelial layers is the principle route for uptake and tissue distribution of IMI [40]. These hydrophobic lipid membranes would act as ion barriers, dramatically reducing the rate of diffusion of the charged guanidine species relative to the parent compound [24]. The toxicity of the guanidine derivatives would be pH dependent: at environmental and physiological pH uptake of the predominately charged species would be significantly limited, thereby mitigating the potential toxic effects of the compounds (Fig. 8).

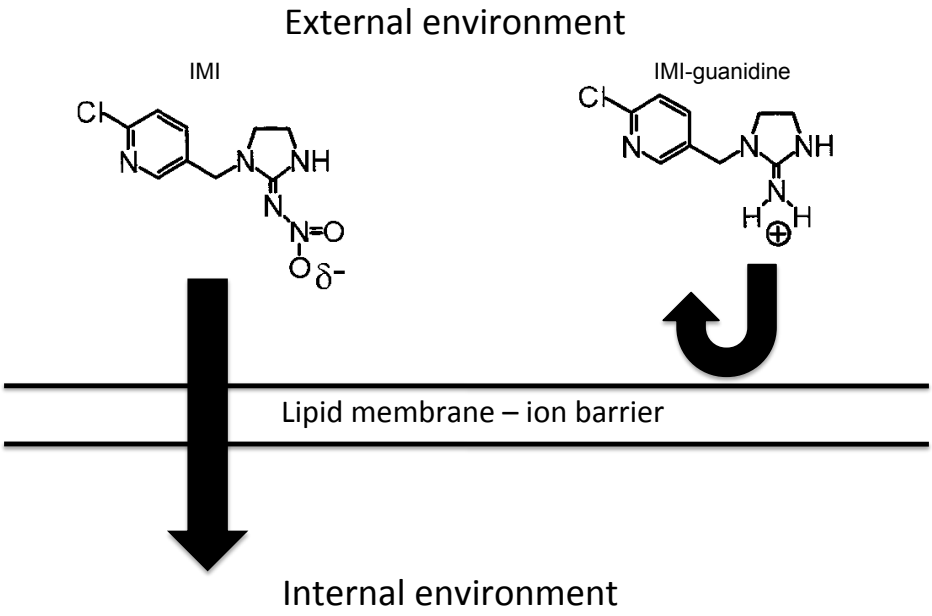

Fig. 8. Relative diffusion of IMI and IMI-guanidine across epithelial layers.

Ammonia is a representative example of a compound displaying pH dependence on toxicity. The pK_a of ammonia ranges from 9 to 10 between 0 °C and 30 °C, respectively. As with the guanidine functional group, the protonated ammonium ion predominates at environmental pH [64]. An examination of the effects of pH on toxicity of ammonia to rainbow trout revealed total ammonia toxicity increased with higher pH [65].

Some mechanisms could potentially influence uptake. One example involves speciation changes at membrane boundaries. The rapid inter-conversion of ionized to un-ionized guanidine species at membrane surfaces – and diffusion of the latter across the membranes – could lead to the development of diffusion gradients and a corresponding increase in uptake of the un-ionized species. Such a mechanism was identified following studies of pH dependence on uptake rates of phenol derivatives in fish. Results showed that actual uptake was greater than predicted from the assumption that uptake was proportional to the un-ionized fractions of the chemical.

Nevertheless, a marked pH dependence on uptake was observed [24]. Although mechanisms such as this could play a role in the uptake of guanidine derivatives, their influence is likely to be minor: the bioavailability of these compounds would be expected to remain low.

In summary, the charge on the guanidine moieties would dramatically reduce the rate of diffusion of these compounds across membranes. The limited bioavailability of these derivatives mitigated concerns associated with their toxicity potential. Given the minimal potential for toxicity to green sturgeon, exposure to the IMI-guanidine and IMI-guanidine-olefin was not characterized.

3. Confirmation of opportunistic feeding

A summation was made of the total number of pits counted each day on the control and treatment beds – including the change in number from the previous day – pre- and post- IMI application (Table 7).

Table 7. Daily sturgeon pit counts and changes from previous day on control (CB) and treatment (TB-N, -C, -S) beds.

		Observation times					
Bed		24 h pre	Application day	24 h post	48 h post	72 h post	96 h post
CB	**Number**	**12**	**10**	**23**	**17**	**13**	**16**
	Change	**N/A**	**-2**	**13**	**-6**	**-4**	**3**
TB-N	Number	15	19	63	54	62	62
	Change	N/A	4	44	-9	8	0
TB-C	Number	9	11	25	26	69	78
	Change	N/A	2	14	1	43	9
TB-S	Number	19	24	36	50	58	65
	Change	N/A	5	12	14	8	7
Total all treatment beds	**Number**	**43**	**54**	**124**	**130**	**189**	**205**
	Change	**N/A**	**11**	**70**	**6**	**59**	**16**

Evidence for preferential feeding by sturgeon on IMI-treated beds was obtained by comparing the cumulative percent change in total pits counted on the initial (24-h pre-application) and final

(96-h post-application) days of observation on each treatment bed relative to the control bed (Fig. 9). The ratios between the increase in pits counted at 24 h pre- and 96 h post-application on the control (33%) and treatment beds TB-N (313%), TB-C (767%) and TB-S (242%) were 9.5, 23.2 and 7.3, respectively, with a mean of 13.3. The ratio between the control bed and all treatment beds combined (377%) was 11.4. These ratios indicate that sturgeon preferentially hunted shrimp on IMI-treated beds relative to non-treated beds.

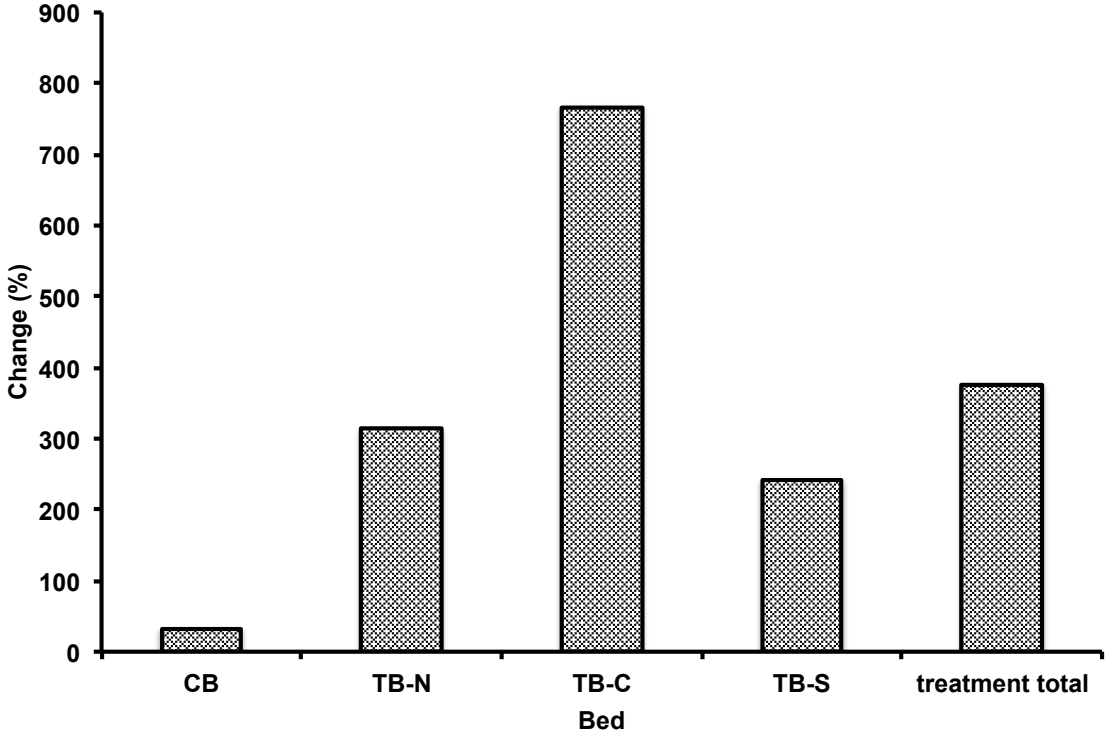

Fig. 9. Cumulative percent change in sturgeon pit counts on control (CB) and treatment (TB-N, -C, -S) bed from initial (24 h pre-) to final (96 h post-application) days of observation.

4. Exposure characterization

(a). IMI concentrations in pore water

No IMI residues were detected in sediment pore water from samples collected pre-application from the control and treatment beds, or post-application from the control bed. Mean

pore water IMI residue concentrations were calculated for the samples collected at each time interval post-application on the treatment beds (Table 8). The approximate LOQ and LOD were 1.0 and 0.3 μg L^{-1}, respectively. The mean background concentration based on the pre-IMI application samples (n = 5) was 0.4 μg L^{-1}. The standard deviation (SD) was 0.1 μg L^{-1}.

Table 8. Mean pore water IMI residue concentrations (SD) for samples collected on treatment beds immediately following application (n = 4 sampling locations) and at latter time intervals post-application (n = 12 sampling locations per time interval). IMI application rate = 0.56 kg a.i. ha^{-1}.

	0 h	24 h	48 h	72 h	96 h
Concentration (μg L^{-1})	42.8 (35.0)	4.5 (4.5)	3.1 (2.9)	6.7 (12.8)	2.2 (1.6)

An exponential equation was fitted to the data points using Excel for interpolation of pore water IMI residue concentrations at any time between 0 – 96 h (Fig. 10).

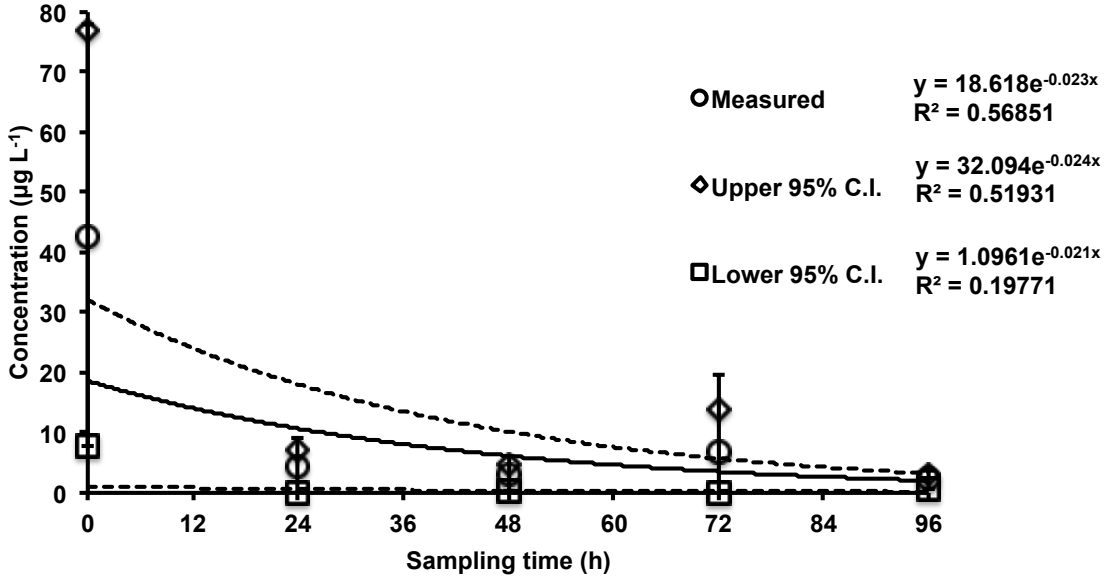

Fig 10. Pore water IMI residue concentration interpolation (error bars = SD) based on mean measured values at time periods 0, 24, 48, 72 and 96 h post-application.

The correlation among data points was low, accounting for only 25% of the variation based on the R^2 value. This was largely due to the high initial value at t = 0. The high concentrations measured at the first time period may have overstated the actual amount of IMI in the pore water. Chemical could have been present on top of the beds that did not percolate into the sediment or flow into open shrimp burrows. Such standing IMI, unincorporated into the underlying sediment, would have been quickly displaced by the incoming tide. Characteristics unique to each sampling location also could have influenced the resulting measured pore water concentrations, as discussed in a subsequent section.

The model adequately described concentrations when compared with the values at 24, 48, 72 and 96 h, however. IMI detected at these latter time points was distributed throughout the sediment; any chemical on the surface had been washed away in previous tidal cycles. Given the influence of these data points on the shape of the overall curve, the value interpolated at t = 0 (18.6 μg L^{-1}), although significantly lower than the mean measured value (42.8 μg L^{-1}), may represent initial pore water concentrations more accurately.

(b). IMI concentrations in burrowing shrimp

The average body mass was calculated for the groups of shrimp (n = 12 per group) collected and analyzed at each sampling period. The mean body mass (SD) at sampling times 24, 48, 72 and 96 h post-IMI application was 8.00 (1.95), 7.66 (1.04), 8.15 (2.03) and 7.64 (1.32) g, respectively. The mean of these averages was 7.86 g with a standard error of the mean (SEM) of 0.13 g. A one-way ANOVA using Excel was applied for comparison of the averages at each sampling time. The null hypothesis that the mean mass was the same for all groups was confirmed (P value = 0.83).

Average IMI concentrations were calculated for the samples collected at each time interval post-application on the treatment beds (Table 9). The approximate LOQ and LOD based on a 4.0x dilution during processing and reconstitution of the samples were 4.0 and 1.2 μg kg^{-1}, respectively. The background IMI concentration for an unexposed shrimp was 2.1 μg kg^{-1}.

Table 9. Mean shrimp IMI residue concentrations (SD) for samples collected on treatment beds at time intervals post-application (n = 12 shrimp; one from each sampling location).

	24 h	48 h	72 h	96 h
Concentration (μg kg^{-1})	22.7 (26.1)	13.5 (17.0)	11.4 (12.2)	7.0 (7.5)

An exponential equation was fitted to the data points using Excel for estimation of shrimp IMI residue concentrations at any time between 24 – 96 h post-application (Fig. 11).

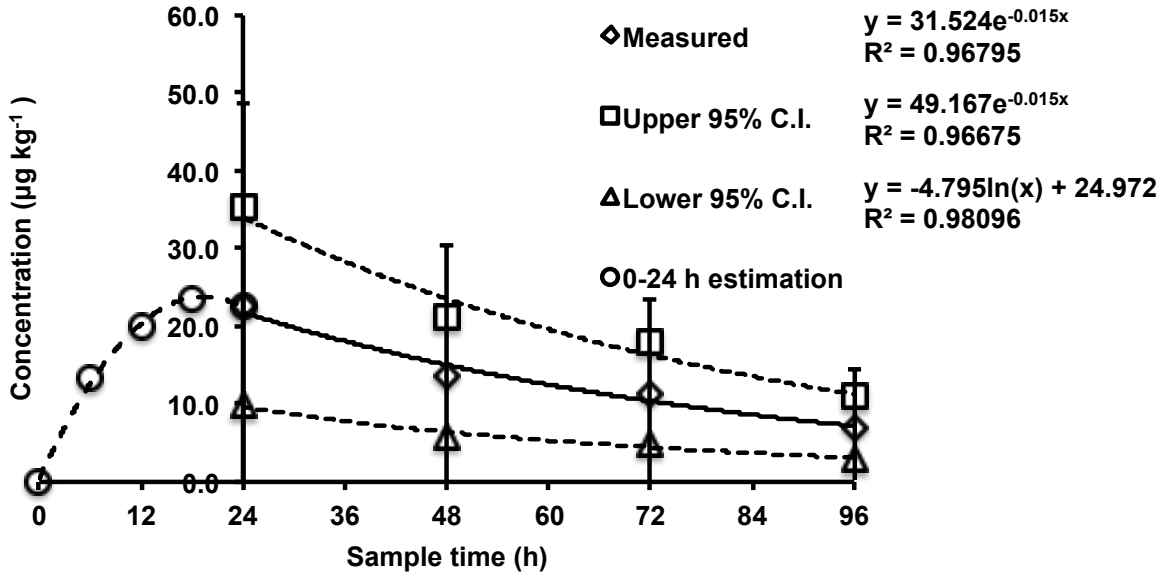

Fig 11. Shrimp IMI residue concentration interpolation (error bars = SD) based on mean of measured values at time periods 0, 24, 48, 72 and 96 h post-application. Values at 6, 12 and 18 h post-application were derived from estimations of pore water concentrations and kinetic modeling in shrimp.

An estimation of IMI residue concentrations in shrimp were included at t = 6, 12 and 18 h – all prior to the first sampling period (t = 24 h). These concentrations were derived from the results of an unpublished depuration study conducted with adult female *N. californiensis*. The static exposures with supplemental aeration were conducted at 47 µg L^{-1} IMI in 30 ppt SW, 18 °C at a loading of 0.8 g wet weight per L test solution. Three groups of shrimp (n = 4 per tank) were exposed for 24 h. At the end of the exposure period shrimp were placed in clean, static SW tanks with supplemental aeration (one tank per group) for depuration times of 0, 24 and 48 h. Shrimp were euthanized following depuration and immediately stored at -80 °C prior to quantitation using LC-MS/MS detection.

The approximate LOQ and LOD based on a 4x dilution during processing and reconstitution of the samples were 4.0 and 1.2 µg kg^{-1}, respectively. The background IMI concentration in an unexposed shrimp was 2.1 µg kg^{-1}. Mean IMI residue concentrations (SD) at depuration times of 0, 24 and 48 h were 84.0 (7.5), 9.5 (5.2) and 2.7 (0.6) µg kg^{-1}, respectively. The 48-h measurements were determined to be non-detects, given the background IMI concentration. These measured values were input into an exposure-time profile for determination of the elimination rate constant (k) and elimination half-life ($t_{1/2}$), with calculated values k = 0.12 h^{-1} and $t_{1/2}$ = 5.8 h. Based on the derived half-life, the 24-h constant-rate exposure approximated four elimination half-lives. This equated to roughly 94% of the plateau level (i.e., the steady state concentration). The steady state concentration was calculated to be 89.0 µg kg^{-1}. The bioconcentration factor (BCF) – the ratio of the steady-state concentration of IMI in the shrimp to the IMI concentration in the water – was estimated at 1.9.

Pore water concentrations were interpolated for t = 6, 12, 18 and 24 h based on the equation of the fitted line $y = 18.618e^{-0.023x}$ at 16.2, 14.1, 12.3 and 10.7 µg L^{-1}, respectively (see Fig. 11).

The mean pore water concentration from time 0 – 24 h was estimated at 14.0 μg L^{-1}. Assuming a constant-rate exposure at this concentration, the corresponding whole body IMI residue concentration in shrimp at steady state based on the estimated BCF was 26.6 μg kg^{-1}. The time intervals 6, 12 and 18 h post-IMI application correlated approximately with 1, 2 and 3 elimination half-lives – representing 50, 75, and 88% of the steady-state IMI concentrations, respectively. The derived IMI concentrations in shrimp were 13.3 μg kg^{-1} (6 h), 20.0 μg kg^{-1} (12 h) and 23.4 (18 h) μg kg^{-1}.

A number of factors made it difficult to estimate IMI concentrations in shrimp at these early time points. These include the minimal number of measurement points used for deriving the elimination half-life from the exposure-time profile, and the uncertainty regarding the actual IMI concentrations shrimp were exposed to in the field. Use of the mean pore water concentration for the 24 h period precluded uptake estimations at the higher pore water concentrations during the initial hours of exposure. This likely underestimated uptake rates and residue concentrations at these early time periods. Such underestimations would have little consequence: as discussed below, residue concentrations in shrimp are not a significant contribution to overall uptake relative to IMI concentrations in pore water.

(c). Experimental bed characteristics

Results from the field studies discussed previously show that green sturgeon feed opportunistically on IMI-impaired shrimp. The relative efficacy of IMI in impairing and killing burrowing shrimp appears coincident with the sediment and bed coverage characteristics. Greater efficacy of IMI in killing shrimp, as measured by the reduction in the number of shrimp burrows observed post-application, has been shown on beds with porous sediments with sparse/no vegetation compared to those with less permeable silty/clay sediments and thick

vegetative cover (K Patten, Washington State University, Long Beach, WA, personal communication). It is hypothesized that IMI binds with greater affinity and does not percolate as rapidly or thoroughly in silty/clay sediments compared with more porous, sandy substrates. Coverage on the beds by native (*Zostera marina*) and/or non-native (*Z. japonica*) eelgrass or other aquatic vegetation may physically block IMI from reaching the surface of the sediment, preventing its incorporation. Additionally, IMI is a plant-systemic [16]. Designed for absorption by plant roots, uptake of IMI could act as another means of reducing overall concentrations of the chemical in the sediment and associated pore water. Finally, chemical could be diluted prior to reaching the sediment by water remaining on the surface in standing pools or flowing swales.

The theoretical maximum initial IMI pore water concentration (assuming 100% of the chemical was incorporated into sediment pore water unbound) was calculated based on the chemical application rate, dimensional parameters of the coring device, the wet weight of the core, and percent moisture of 25% (which was determined from a comparable sediment sample collected following a subsequent IMI test application in July 2012) (Table 10).

Table 10. Input values and calculated theoretical maximum initial IMI concentration in pore water.

Application rate (kg. a.i. per ha)	0.56
Core diameter (cm)	10.2
Depth of core (cm)	63.5
Amt. IMI per core volume (µg)	457.7
Wet weight of core (g)	9761
Percent moisture	25%
Fraction of IMI in pore water	100%
Pore water IMI conc. (µg L^{-1})	**187.6**

The theoretical maximum concentration of 187.6 µg L^{-1} was 4-fold greater than the mean measured value (42.8 µg L^{-1}), and 2-fold more than the highest sampling point measured (88.3

μg L^{-1}). Assuming the accuracy of the calculation, several factors could account for measured values in pore water at t = 0 being lower than the theoretical maximum. Chief among these was the likelihood that any chemical that did not incorporate into the sediment prior to the incoming tide was washed away. Additionally, characteristics varied among sampling locations on the control and treatment beds. The features discussed above could have had an influence on the amount of IMI that successfully incorporated into the sediment.

IMI was applied to the beds via jet agitator connected to the back of an ATV at a target application rate of 0.56 kg a.i. ha^{-1} (K Patten, Washington State University, Long Beach, WA, personal communication). Despite careful alignment of the application corridors, deviations may have occurred due to the influence of wind or incidental application overlaps or omissions. It was assumed that the target application rate was realized at all sampling locations on the treatment beds.

Sediment compositions, defined by the percent retained following filtration according to particle grain size as sand/silt/clay from the two core samples taken from TB-N-2 and TB-S-2 were 89.7/5.5/4.8 and 92.9/3.1/4.0, respectively. The total percent of solids were 80.5 (TB-N-2) and 79.6 (TB-S-2). Organic carbon measurements included the percent of total in the sediment and the concentration (mg L^{-1}) dissolved in the pore water: 0.704% and 29.8 (TB-N-2), 0.300% and 22.1 (TB-S-2). The percent moisture for both samples – calculated as the differences between wet and dry weights – was 18.8 (TB-N-2) and 20.1 (TB-S-2).

IMI residues were quantitated in isolated pore water and dried sediment by the contract laboratory (PAL) on a sediment sample collected following a subsequent test application at a comparable location to the July 2012 test beds discussed previously. Bound IMI, as a percent of total, was 66.7. Assuming the target application rate of 0.56 kg a.i. ha^{-1} was achieved, this result

confirmed that sediment binding – perhaps attributed to organic carbon – was a significant factor in the observed difference between theoretical and measured IMI residue concentrations in pore water.

The percentage of vegetative cover was estimated within a 5 m radius of the center of each treatment bed sampling location (Table 11).

Table 11. Percentage of vegetative cover around treatment bed sampling locations.

Sampling location	Vegetative cover (%)	Sampling location	Vegetative cover (%)
TB-N-1	90	TB-C-1	30
TB-N-2	95	TB-C-2	20
TB-N-3	100	TB-C-3	0
TB-S-1	5	TB-C-4	15
TB-S-2	75	TB-C-5	1
TB-S-3	70	TB-C-6	20

The mean coverage at treatment sampling locations (SD) across all beds was 43 (39)%, varying widely among locations.

The mean water depth was estimated at the sampling locations during low tide (Table 12).

Table 12. Water depth range at sampling locations during low tide.

Sampling location	Water depth range (cm)	Sampling location	Water depth range (cm)
TB-N-1	dry	TB-C-1	dry
TB-N-2	dry	TB-C-2	dry
TB-N-3	dry	TB-C-3	1-3
TB-S-1	4-5	TB-C-4	dry
TB-S-2	1-2	TB-C-5	2-4
TB-S-3	dry	TB-C-6	1-3

Location TB-S-1 was situated in the center of a swale. The remaining locations were either dry or under shallow pools of standing water.

IMI residues in pore water were quantitated at four locations sampled shortly after application of the chemical, prior to the first incoming tide. Results were compared along with the vegetative and water coverage at the respective sample sites (Table 13). The approximate LOQ and LOD were 1.0 and 0.3 μg L^{-1}, respectively. The mean background concentration (SD) based on the pre-IMI application samples (n = 5) was 0.4 (0.1) μg L^{-1}.

Table 13. Influence of vegetative cover and water on beds with IMI residue concentrations in pore water at locations sampled shortly after application of the chemical prior to the first incoming tide (application rate = 0.56 kg a.i. ha^{-1}).

Sampling location	Vegetative cover (%)	Water depth range (cm)	IMI conc. (μg L^{-1})
TB-N-2	95	dry	52.4
TB-C-4	15	dry	88.3
TB-C-5	≤ 1	2-4	18.4
TB-S-1	5	4-5	12.3

IMI residue concentrations in pore water were inversely related with vegetative cover: the high coverage at TB-N-2 relative to TB-C-4 correlated with lower IMI concentrations in the former compared with the latter. The sampling locations on completely dry beds (TB-N-2 and TB-C-4) had pore water IMI residue concentrations that were significantly higher than the two beds with water (TB-C-5 and TB-S-1). There is no certainty that such features would compromise efficacy, however. No recordings were made of burrowing shrimp control efficacy around the individual sampling locations (only overall efficacy on each test bed was measured).

(d). Worst-case exposures

Results from the comparison of pit counts between control and IMI-treated beds indicated preferential feeding by green sturgeon on chemically impaired shrimp. Estimations were made of the extent of exposure to IMI received by green sturgeon during their foraging on these beds. Several assumptions – along with variants of key parameters – were made when calculating the different exposure scenarios. With no data on actual feeding behavior and consumption rates, all of the estimates were intentionally liberal, and likely overestimated the actual values. The general assumptions were as follows.

In order to ensure a reasonable depth for sturgeon to swim onto the beds, the feeding window was established at ± 2 h from peak high tide. The IMI concentrations in pore water and shrimp throughout the entire foraging window were assumed equivalent to the values at the median time points as interpolated in Figures 10 and 11, respectively.

Sturgeon were assumed to be exposed to IMI at concentrations in the pore water, without dilution from the water above the sediment, for the entire 4 h duration of the tidal feeding. The availability of shrimp for consumption was deemed limitless. Additionally, it was supposed that sturgeon would feed *ad libitum* at a daily rate of 12% body mass – the maximum ration measured in 2.4 g juvenile white sturgeon in a study of food consumption and growth [66]. The allocation of food energy to growth and metabolism differs in adult and juvenile fish. The energy requirements needed for growth in adult sturgeon would be less than in juveniles [67]. A feeding rate of 12% body mass per day likely overestimates actual consumption in adult green sturgeon.

The average green sturgeon body mass (as determined in measurements in fish collected during environmental monitoring) was 13.5 kg. The average shrimp body mass, as discussed

previously, was 7.9 g. It was estimated that sturgeon would consume their entire daily ration of shrimp during one foraging period. Based on the estimated daily feeding rate of 12% body mass, the total mass of shrimp consumed per tidal feeding period was estimated at 1.62 kg – approximately 205 shrimp.

Shrimp bed populations could support such feeding assumptions. Highly populated shrimp beds had average measured densities of 130 shrimp m^{-2} [68]. Average pit diameter was estimated at 0.56 m based on a pit area of 0.25 m^2 [21]. The depth to which sturgeon dug was unknown (due to the loose substrate, pits partially filled in soon after being dug). Owing to their extended mouths coupled with their suction of the surrounding pore water, sturgeon would likely be able to extract shrimp from a considerable depth, however. An assumption was made that sturgeon successfully captured shrimp from the entire depth of their burrows (0.6 – 0.9 m) [69].

Peak pore water concentration. A scenario was modeled to reflect a worst-case exposure at peak pore water IMI residue concentrations interpolated from the measured pore water values while feeding at the rate estimated above, as summarized below (Table 14).

Table 14. Summary of bed features and inputs in a worst-case sturgeon IMI exposure at peak pore water residue concentration occurring 6 h post-application (0.56 kg a.i. ha^{-1}).

Avg. sturgeon mass (kg)	13.5
Avg. predation time (h)	4
Avg. pore water IMI residue conc. (µg L^{-1})	27.8
Total mass of shrimp consumed (kg)	1.62
Avg. shrimp IMI residue conc. (µg kg^{-1})	13.3

Two tidal cycles had passed prior to pore water and shrimp samplings at 24 h post-IMI application. Based on the pore water data interpolation illustrated in Fig. 10, the highest mean IMI residue concentration occurred at the first high tide feeding window, 6 h post-treatment.

Incorporating the equation of the line for the upper 95% C.I., the corresponding mean pore water concentration was calculated at 27.8 µg L^{-1}. The estimated shrimp IMI residue concentration at 6 h post-treatment was 13.3 µg kg^{-1}.

Peak shrimp residue concentrations. A scenario was modeled to reflect a worst-case exposure to green sturgeon while feeding at peak shrimp IMI residue concentrations, as summarized below (Table 15).

Table 15. Summary of bed features and inputs in a worst-case sturgeon IMI exposure at peak shrimp residue concentration occurring 30 h post-application (0.56 kg a.i. ha^{-1}).

Avg. sturgeon mass (kg)	13.5
Avg. predation time (h)	4
Avg. pore water IMI residue conc. (µg L^{-1})	15.6
Total mass of shrimp consumed (kg)	1.62
Avg. shrimp IMI residue conc. (µg kg^{-1})	31.4

The highest measured IMI residue concentrations in shrimp were at the first sampling time, 24 h post-application. Residue concentrations were modeled based on kinetic data for the previous high tide feeding time (18 h) and by interpolation of measured values for the succeeding high tide (30 h). The latter time period was chosen due to greater confidence in the predicted concentration derived from an interpolation based on measured values coupled with the high correlation of the modeled line. Incorporating the equation of the line for the upper 95% C.I., the corresponding mean shrimp IMI residue concentration was calculated at 31.4 µg kg^{-1}. The corresponding mean pore water concentration, determined through interpolation of the equation of the line for the upper 95% C.I., was 15.6 µg L^{-1}. All other assumptions and variables were identical to the pore water exposure discussed above.

5. *Exposure verification*

IMI residues were quantitated in plasma from one sturgeon at 18 h pre-application, and 20 sturgeon 30 h post-application using LC-MS/MS detection. The approximate LOQ and LOD, based on the 2.5x dilution following reconstitution of the samples, were 2.5 and 0.8 μg kg^{-1}, respectively. No IMI residues were detected in either the pre- or post-application samples.

6. Uptake estimation

(a). Branchial uptake

The functions of fish gills include respiratory gas exchange, osmoregulation, nitrogen excretion and control of acid-base balance. These physiological features also result in the movement of xenobiotics, such as IMI, across the gills [24]. The fundamental components of the gills are the arches, filaments and lamellae. Gill arches are aligned along either side of the pharyngeal cavity. Water is channeled between the arches directionally through the pharynx, exiting at the opercula. Two branches of filaments extend posterior from each arch. Within the filaments lie the lamellae; structures responsible for the transfer of gasses between blood and water. Water flows between these tightly spaced structures. Blood flow in the lamellae is opposite to the flow of water. This arrangement results in an efficient counter-current exchange between blood and water [67].

The most important factors in estimating branchial uptake are blood:water partitioning, gill diffusional resistance, cardiac output and respiratory volume [51]. As addressed in the introduction, IMI is a small (MW = 255.7), relatively polar (log K_{ow} = 0.57), uncharged compound at environmental and physiological pH. These features suggest that passive diffusion would be the principal mechanism of transport across epithelial layers. Moreover, given its low

log K_{ow} value, branchial uptake of IMI is likely to be rate-limited by the capacity of blood to remove chemical from the gills [24, 51, 70, 71]. Diffusional resistance to the transport of IMI across membranes was assumed to be minimal relative to the capacity of water and blood to deliver and remove chemical, respectively [51, 71].

Branchial uptake of IMI in green sturgeon was estimated under the conditions for a worst-case pore water exposure discussed above. The concentration of IMI available for uptake was assumed to be the free, unbound fraction measured in sediment pore water. Chemical adsorbed to sediment and/or organic carbon would not be available for uptake. No account was made for possible changes in water chemistry at the gill membrane surface. It was also assumed that sturgeon would be exposed to the concentration of IMI calculated in the pore water without dilution from the overlying water column during foraging.

The uptake rate constant predicted by the flow-limited gill model for chemicals with a log $K_{ow} < 1$ was 1.6 L kg^{-1} h^{-1}. Input values and the calculated branchial IMI absorption are summarized below (Table 16).

Table 16. Input values and calculated branchial uptake of IMI following worst-case pore water exposure.

Exposure time (h)	4
IMI conc. (µg L^{-1})	27.8
Uptake rate (L kg^{-1} h^{-1})	1.6
Avg. branchial IMI uptake (µg kg^{-1})	**177.9**

In validation studies with RBT, the predicted chemical uptake based on the flow-limited model overestimated observed values by an average of 30% [51]. This difference is likely due to diffusion resistance not accounted for in the model. The results stated above should be

considered an upper limit to exchange rates: any diffusion resistance would only lower overall branchial uptake of IMI.

(b). Dietary uptake

Dietary uptake of IMI would result from gastrointestinal (GIT) absorption of the chemical following consumption of contaminated shrimp. Although significant structural differences and diverse characteristics such as pH, fluid flux, membrane transport, and enzymatic systems exist between species, the absorption of xenobiotics follows the generalized processes outlined below [24].

The absorptive availability of a chemical necessitates the breakdown of the surrounding food within the gut lumen. The rate of uptake across the intestinal epithelial into enterocytes depends on the physicochemical properties of the compound. Highly lipophilic chemicals would be associated in mixed micelles; those more polar could diffuse unassociated across the gut epithelium. Other chemicals could mimic endogenous ligands for membrane transport proteins on the apical surface, facilitating transport of these compounds from the gut lumen into the enterocytes. Two mechanisms could play a role in reducing concentrations of the chemical within enterocytes: efflux transporters on the apical side could return chemical to the lumen, while biotransformation enzymes could metabolize the chemical – a process known as gut wall loss. Ultimate uptake into the blood would occur via passive diffusion and/or facilitated transport across the basolateral membrane of the enterocytes. First-pass loss – metabolism/biliary excretion of chemical entering the liver via the portal vein prior to reaching general circulation – could limit overall systemic uptake [24, 67, 72].

Due to uncertainties with application of dietary uptake models, including species and physicochemical extrapolations, AE was conservatively estimated at 100%. Input values and the

calculated dietary IMI absorption are summarized below (Table 17). No account was made for potential uptake of IMI from pore water or bound sediment swallowed during consumption of shrimp.

Table 17. Input values and calculated dietary uptake of IMI following worst-case shrimp exposure.

Total mass of shrimp consumed (kg)	1.62
Avg. IMI conc. per shrimp (μg kg^{-1})	31.4
Avg. stugeon mass (kg)	13.5
Assimilation efficiency (%)	100.0
Avg. dietary IMI uptake (μg kg^{-1})	**3.8**

(c). Total IMI uptake

Branchial uptake from pore water would account for most of the systemic absorption of IMI. A comparison of results between the worst-case pore water and shrimp consumption models indicated that branchial uptake (177.9 μg per kg body weight) was 47-fold greater than dietary uptake (3.8 μg per kg body weight). Comparisons of uptake within each of the models revealed similarly distorted contributions among uptake routes. Shrimp IMI residue concentrations corresponding with the highest pore water concentrations 6 h post-application were 13.3 μg kg^{-1}, resulting in dietary uptake of 1.6 μg per kg body weight. Branchial uptake (177.9 μg per kg body weight) was 111-fold greater. Even at the highest shrimp IMI residue concentrations measured at 30 h post-application (31.4 μg kg^{-1}, dietary uptake rate of 3.8 μg per kg body weight), branchial uptake would far exceed dietary uptake. The pore water IMI residue concentrations at 30 h were 15.6 μg L^{-1}, corresponding with branchial uptake of 99.8 μg kg^{-1}. This would result in a 26-fold greater contribution than dietary uptake to overall IMI systemic absorption.

7. White sturgeon controlled exposure studies

(a). Sturgeon sensitivity to IMI

The percent mortalities at 96, 139 and 202 mg L^{-1} IMI at the conclusion of the 96-h exposure were 20, 60 and 100, respectively. There were no mortalities at the 46 or 66 mg L^{-1} IMI concentrations. All controls were alive and in normal condition at the end of the experiment. Statistical software (SPSS for Mac v.18, Softonic Int'l) was used for development of the concentration-response curve (Fig. 12).

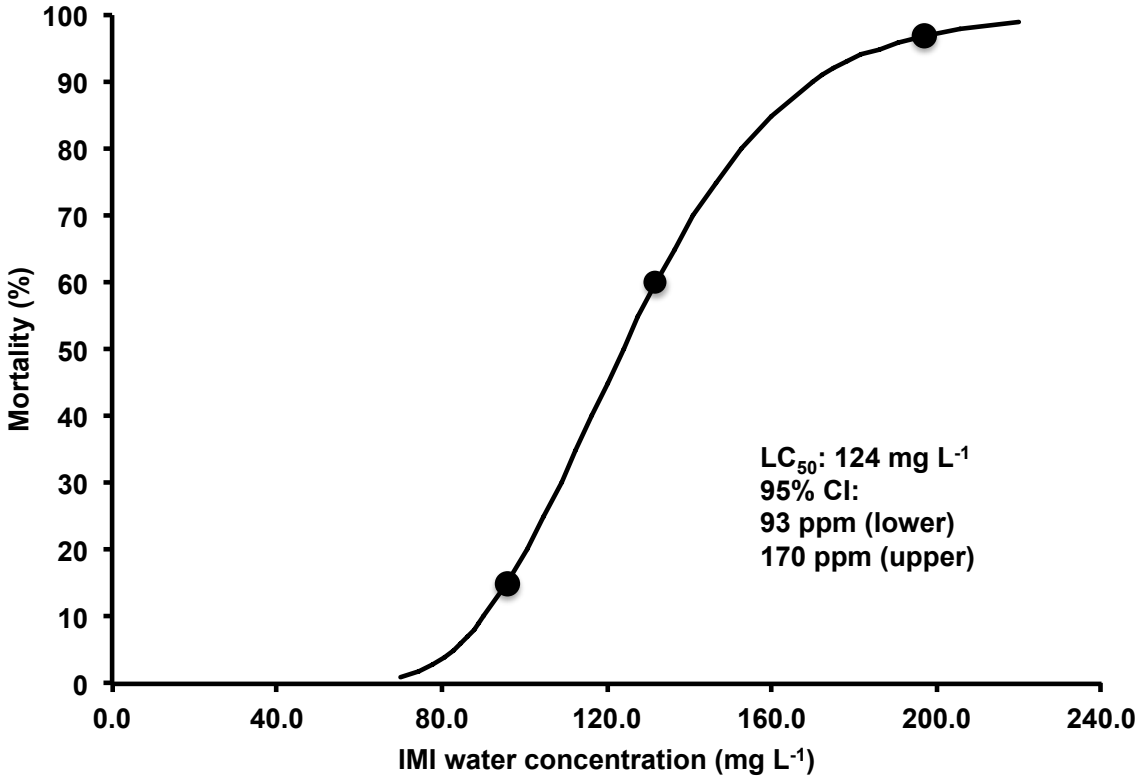

Fig. 12. Concentration-response curve for 96-h IMI FW exposure to juvenile white sturgeon.

The interpolated 96-h LC_{50} was 124 mg L^{-1}. The 95% confidence intervals were relatively broad due to the limited number of test organisms (n = 5 per concentration). A comparison was

made with the published LC_{50} for juvenile RBT, another cold water species (211 mg L^{-1}) [13]. The difference was minimal, indicating that white sturgeon – and by extension green sturgeon – do not appear to exhibit extreme sensitivity to IMI. As determined by the characterization discussed previously, the IMI exposure scenario modeled for determination of the 96-h LC_{50} does not reflect that which would be expected in the field: the durations of exposure were much longer and the concentrations were orders of magnitude greater for the 96-h median lethal toxicity test.

(b). Simulated field exposures and plasma residue concentrations

The contract laboratory (PAL) conducted analytical confirmation of the IMI concentrations in the test SW. Measured IMI concentrations corresponding to the nominal values at the 2.2 kg a.i. ha^{-1} application rate of 678, 100 and 15 µg L^{-1} at 6, 18 and 30 h were 477, 97.5 and 19 µg L^{-1}, respectively. Measured IMI concentrations corresponding to the nominal values of 169, 25 and 4 µg L^{-1} at 6, 18 and 30 h at the 0.56 kg a.i. ha^{-1} application rate were 154, 24, and 2.7 µg L^{-1}, respectively.

Plasma IMI residue concentrations were quantitated in juvenile white sturgeon following controlled exposures based on estimated pore water concentrations following the earlier sediment sample collection in July 2010 at the 2.2 kg a.i. ha^{-1} application rate. Plasma residues were quantitated using both LC-MS/MS (1^{st} simulated high tide) and ELISA (2^{nd} and 3^{rd} simulated high tides) detection (Table 18). The approximate LOQ and LOD for LC-MS/MS, based on a 4.5x dilution during processing and reconstitution of the samples, were 4.5 and 1.4 µg kg^{-1} respectively, with an average background IMI concentration (unexposed controls, n = 2) of 2.8 µg kg^{-1}. The ELISA LOQ and LOD were approximately 4.0 and 1.4 µg kg^{-1}, respectively,

with an average background IMI concentration (unexposed controls, n = 3) of 1.8 μg kg^{-1} (SD = 0.1 μg kg^{-1}).

Table 18. Mean plasma IMI residue concentrations and standard deviations following the initial high tide exposure (LC-MS/MS detection, n = 4) and subsequent recovery/exposures (ELISA detection, n = 6 and 4, respectively) at the 2.2 kg a.i. ha^{-1} application rate.

Exposure period(s)	Concentration (μg kg^{-1})	SD (μg kg^{-1})
1st high tide	20.7	3.0
2nd high tide	32.7	3.7
3rd high tide	32.7	8.6

The WGHOGA is currently seeking a National Pollutant Discharge Elimination System (NPDES) permit for IMI at the 0.56 kg a.i. ha^{-1} application rate only (the USEPA has granted registration to the growers at this application rate, dated 6 June 2013). Given the higher exposure concentration employed in this experiment, the resulting plasma IMI residue values likely would be significantly higher than levels found in green sturgeon during environmental monitoring. Additionally, the concentrations calculated using ELISA detection at the latter two time series might have overestimated actual IMI residues due to possible cross-reactivity with several metabolites [38, 55].

Average plasma residue concentrations were calculated for the samples following the IMI exposure scenarios at the 0.56 kg a.i. ha^{-1} application rate using LC-MS/MS detection (Table 19). The approximate LOQ and LOD, based on a 4.5x dilution during processing and reconstitution of the samples, were 4.5 and 1.4 μg kg^{-1} respectively, with an average background IMI concentration (unexposed control, n = 1) of 2.1 μg kg^{-1}.

Table 19. Mean plasma IMI residue concentrations and standard deviations following the initial high tide exposure and subsequent recovery/exposures (n = 3 ea) at the 0.56 kg a.i. ha^{-1} application rate.

Exposure period(s)	Concentration (µg kg^{-1})	SD (µg kg^{-1})
1st high tide	11.8	2.3
2nd high tide	8.2	1.2
3rd high tide	8.6	2.0

Based on the results of the exposure characterization discussed above, the concentrations and durations used in this worst-case water-only exposure scenario were greater than green sturgeon are expected to encounter in the field. These reported plasma IMI residue concentrations should overestimate the highest concentrations that would be measured in green sturgeon following environmental monitoring and would represent a ceiling for expected concentrations.

The plasma isolation procedure was outside of standard protocol [73]. The need for prompt processing of large numbers and volumes of blood necessitated the use of a large capacity centrifuge. Although able to handle 15 mL aliquots, the centrifuge that was used had a maximum relative centrifugal force (RCF) of 1900 x *g* – slightly lower than the RCF of 2000 x *g* recommended for obtaining platelet-rich plasma. The light spin protocol that was used (1900 x *g*, 10 min.) produced a cloudy upper plasma layer and a defined bottom red cell layer. The buffy coat layer composed of white blood cells and larger platelets was undefined in many of the centrifugations, however [73]. The plasma samples used for IMI residue analysis may have contained fractions of these leukocytes and platelets due to the incomplete isolation during the centrifugation procedure (time constraints prevented a second sample centrifugation). The presence of additional blood components may have influenced total IMI residue concentrations due to the potential binding of chemical. Since separation was inconsistent, the effect on residue concentrations could have varied across the samples analyzed (similarly, this may have affected the results from the depuration study discussed below).

(c). Persistence of IMI in sturgeon

Plasma IMI residues were quantitated at chosen depuration time periods using LC-MS/MS detection (Table 20). The approximate LOQ and LOD were the same as the simulated field exposure at the 0.56 kg a.i. ha^{-1} application rate.

Table 20. Mean plasma IMI residue concentrations and standard deviations at depuration times following a 678 µg L^{-1} IMI 6h static water exposure (estimated uptake = 6.5 mg kg^{-1}), n = 4 ea.

Recovery time (h)	Concentration (µg kg^{-1})	SD (µg kg^{-1})
0	20.7	3.0
4	25.2	6.2
16	20.4	0.4
32	23.2	8.7

Against expectations, there was no discernable loss of IMI over the 32-h depuration period. Potential reasons for this included biological variability influencing the results within and among sample groups, an insufficient length of recovery time for determining the elimination half-life in sturgeon, and non-ideal plasma isolation.

A range of residue concentrations would be expected based on individual differences in IMI uptake and elimination. Such variability decreases with a corresponding increase in sample size. The mean residue concentrations calculated for each group may not have been representative of the population means due to the small sample sizes (n = 4) incorporated. The RSD for each group at depurations t = 0, 4, 16, and 32 h were 14.7, 24.7, 2.0 and 37.7%, respectively. Assuming elimination of IMI follows an unimodal distribution, a RSD of 10% or less would be considered low, 25% or greater high [72]. Moderate (t = 0 h) and high (t = 4, 32 h) variability measured in these groups suggests they may not have been representative of the population means; mean concentrations could have been to either the left (lower) or the right (higher) of the normal population distribution.

The elimination half-life of IMI in sturgeon was likely considerably longer than 32 h – the length of the experimental depuration period. A relatively low rate of loss of IMI, coupled with the inherent variability within groups, would have limited the ability for detecting loss over the short time period: if elimination of IMI was relatively slow, small decreases in concentration over the measurement times could have been masked by the variability within the groups.

Sample size was limited due to time and loading constraints. The average mass allowed only four fish per tank in order to maintain USEPA-prescribed load limitations for the static 6-h exposures. Additionally, the logistics for handling a greater number of fish throughout the depuration periods would have required additional tanks and personnel, neither of which was available.

The experimental design was also influenced by the limited information on IMI. Without the availability of PK studies in fish, the behavior of the chemical in sturgeon was estimated based on reports in other animals. An 80 min elimination half-life was reported for mice [28]. This value was based on measured plasma residue concentrations relative to the maximum level at sampling time t = 15 min post-intraperitoneal (i.p.) injection. The successive measured plasma residue concentrations used for determination of the elimination half-life likely encompassed the distributional phase of the chemical, however. A graphical representation of the data points revealed the bi-phasic elimination of IMI in mice. Following distributional equilibrium, the elimination of IMI during the terminal phase would have been longer [72].

The routes of elimination – including the contribution of metabolism – were unknown in fish. Over 50% of the chemical – greater than half of which were present as metabolites – was recovered in the urine collected 0-24 h post-i.p. injection in mice [28]. Metabolic pathways for IMI have been identified in several mammalian species [31-35]. It was unknown what

contribution metabolism would have on overall elimination of IMI in sturgeon, however. Without rudimentary knowledge of IMI elimination in fish, a conservative depuration time based on the mammalian data was constructed. In hindsight, this may have underestimated the terminal phase elimination half-life in sturgeon.

Despite the limitations with the experimental design and plasma isolation, the data were suggestive of an elimination half-life in sturgeon greater than 32 h – significantly longer in fish than observed in mammals. The terminal elimination half-lives determined in the toxicokinetics studies with RBT discussed below supported the white sturgeon results.

Mean IMI residue concentrations were calculated in tissues from fish at 32 h depuration (Table 21). The approximate LOQ and LOD, based on a 2.5x dilution during processing and reconstitution of the samples, were 2.5 and 0.8 μg kg^{-1}, respectively. The background concentrations measured in clean control tissue samples (n = 1 ea.) were as follows: 2.4 μg kg^{-1} (brain), 1.7 μg kg^{-1} (liver) and 2.6 μg kg^{-1} (white muscle).

Table 21. Mean tissue IMI residue concentrations and tissue:plasma ratios (SD) from white sturgeon at 32 h depuration following a 678 μg L^{-1} IMI 6 h static water exposure, n = 4 ea.

Tissue	Concentration (μg kg^{-1})	Tissue:plasma ratio
Brain	26.5 (5.0)	1.2 (0.2)
Liver	47.1 (12.6)	2.1 (0.3)
White muscle	26.3 (3.3)	1.2 (0.2)

The mean IMI residue concentration (SD) in bile from fish at 32 h depuration (n = 4) was 48.0 (10.5) μg kg^{-1}. The approximate LOQ and LOD, based on a 2.5x dilution during processing and reconstitution of the samples, were 2.5 and 0.8 μg kg^{-1}. The background concentration measured in a clean control bile sample was 0.4 μg kg^{-1}.

The tissue:plasma ratios and bile concentration were compared with those measured from the RBT studies. Comparisons between species and interpretation of the results are addressed below.

8. Rainbow trout toxicokinetics studies

(a). Preliminary depuration study

Plasma IMI residues were quantitated in samples at all four post-injection time periods (Table 22). The approximate LOQ and LOD were 1.0 and 0.3 μg kg^{-1}, respectively.

Table 22. Mean plasma IMI residue concentrations (SD) from RBT at sampling periods t = 1, 4, 10, 24 h post-IMI bolus injection (n = 4, 4, 3, 3, respectively).

Depuration time post-injection (h)	Concentration (μg kg^{-1})
1	151.8 (10.6)
4	125.2 (42.1)
10	77.8 (46.0)
24	53.6 (22.4)

The theoretical plasma concentration immediately after injection (C_0) prior to distribution of the chemical to body tissues was estimated at 4800 μg kg^{-1} based on a plasma volume equivalency of 4% body mass [74]. The mean plasma concentration at t = 1 h post-injection was approximately 3% of the theoretical C_0 value. This was indicative of extensive distribution of IMI throughout the fish: given the apparent long elimination half-life evidenced in the aforementioned white sturgeon depuration study, significant elimination of chemical from the body was unlikely.

The limited number of sampling periods along with biological variability within periods due to small sample sizes hindered accurate estimation of the primary PK parameters. Derivation of the terminal phase elimination rate constant (k) and half-life ($t_{½}$) from a concentration-time

profile was not possible: no accurate prediction could be made for the separation of the distributional and terminal phases, nor was the final depuration time (24 h) sufficient for adequately defining the slope of the terminal phase [72]. Additional tissues (brain, kidney, liver and white muscle) were not analyzed because of these limitations.

Valuable insight was gained from the study, however. Plasma IMI residue concentrations were well above the LOQ for LC-MS/MS detection. This allowed for tailoring of the experimental design for the definitive study by extending the length of the depuration sampling times and use of an additional low IMI bolus concentration.

(b). Definitive depuration study

The intended nominal concentrations for the low and high doses were 25.0 and 250.0 mg L^{-1}, corresponding to i.a. bolus dose injections of 25.0 and 250.0 μg kg^{-1}. Measured concentrations of the dose preparations using LC-MS/MS detection were 47.6 mg L^{-1} (low dose) and 232.7 mg L^{-1} (high dose). A review of the laboratory notes revealed an error in preparation of the low dose. The nominal concentration following re-calculation was 44.7 mg L^{-1}. The modeling of plasma concentrations for the estimation of PK parameters was based on the low and high nominal doses of 44.7 and 250.0 μg kg^{-1}, respectively. Theoretical plasma concentrations for the low and high dosing groups at C_0 based on a plasma volume equivalency of 4% body mass immediately after injection prior to distribution of the chemical to body tissues were 1117.5 and 6250.0 μg kg^{-1}, respectively [74].

Mean plasma IMI residue concentrations and standard deviations were calculated for the low and high dose samples at all periods following bolus i.a. injections (Table 23). The approximate LOQ and LOD based on a 4.5x dilution during processing and reconstitution of the samples were 4.5 and 1.4 μg kg^{-1}, respectively. The mean background concentrations (SD) in plasma samples

measured pre-IMI injection were 4.0 (1.2) μg kg^{-1} (low dose, n = 4), and 6.7 (1.7) μg kg^{-1} (high dose, n = 5).

Table 23. Mean plasma IMI residue concentrations (SD) from low and high dose RBT post-IMI bolus injection, n = 5 replicates except t = 16 low dose (n = 2).

Time (h)	Concentration (μg kg^{-1})	
	Low dose	High dose
1	195.3 (106.9)	412.9 (96.3)
2	82.3 (15.3)	153.9 (10.8)
4	31.2 (7.0)	131.9 (16.4)
8	20.3 (3.8)	117.2 (13.4)
16	19.5*	105.0 (15.4)
24	15.2 (2.7)	93.6 (14.8)
36	14.3 (3.1)	82.2 (12.9)
48	13.3 (2.9)	76.4 (8.1)

The measured plasma residue concentrations at the first sampling period (1 h) relative to the theoretical C_0 values were approximately 17.5 and 6.6% for the low and high doses, respectively. Comparable to the preliminary depuration study, these measures were indicative of extensive distribution of IMI throughout the body. The high variances measured at both dosing levels at the initial sampling period (t = 1 h) may have been influenced by incomplete flushing of the catheter in some fish following injection of the IMI dose: residues that remained in the catheter may have been collected along with the withdrawn blood, artificially elevating actual concentrations.

Mean plasma IMI residue concentration-time profiles were developed for both the low and high dose samples (Fig. 13). Both profiles revealed rapid initial drops in IMI concentrations followed by slower declines at latter time points. These patterns suggest the existence of an early distributional phase followed by a log-linear terminal elimination phase. The limited

number of data points at the earlier time periods made it difficult to clearly define these two phases, however. This precluded application of a two-compartment model for determining the kinetic parameters.

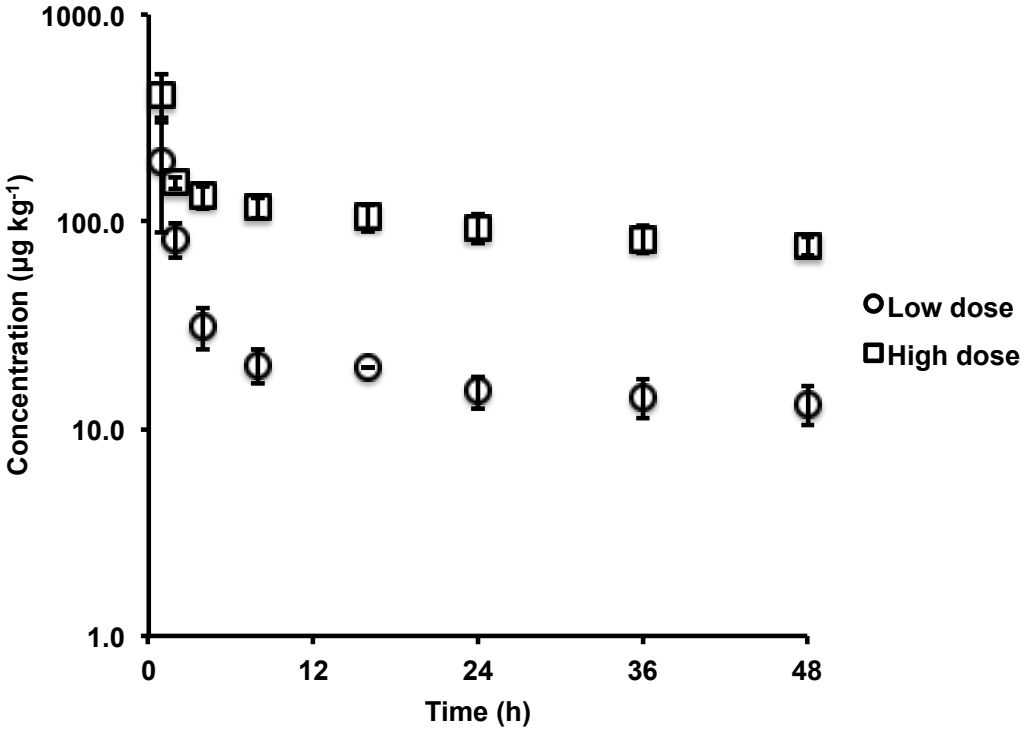

Fig. 13. Log-transformed plasma concentration-time profiles for low and high dose RBT following bolus i.a. injections of IMI. Data points are the sample means ± SD (n = 5 ea.) except low dose t = 16 (n = 2).

Non-compartmental analysis was used for estimation of the kinetic parameters (WinNonlin, Pharsight). Based on the elimination profiles, it was assumed that the distributional phase was relatively fast. Time points 8, 16, 24, 36 and 48 h were therefore specified for estimation of terminal half-life within the model. The primary TK parameters along with the elimination half-life were calculated for each individual (Table 24).

Table 24. Primary kinetic parameter estimations for RBT injected with a low (44.7 μg kg^{-1}) or high (250.0 μg kg^{-1}) dose of IMI. V_{ss} (%TBW) was calculated based on RBT total body water (TBW) of 714 ml kg^{-1} [75].

	Low dose samples				
Parameter	L2	L3	L4	L5	L6
$AUC_{0-\infty}$ (h μg L^{-1})	2332.5	1573.5	3522.8	3011.6	1640.9
$AUC_{0-48\,h}$ (h μg L^{-1})	1154.3	904.4	1381	1086.8	952.8
V_{ss} (mL kg^{-1})	1565.3	1619.8	1498.2	1632.4	1493.7
V_{ss} (% TBW)	219	227	210	229	209
CL_B (mL h^{-1} kg^{-1})	19.2	28.4	12.7	14.8	27.2
$t_{½}$ (h)	68.6	45	94.6	78.5	41.5
	High dose samples				
Parameter	H1	H2	H4	H5	H6
$AUC_{0-\infty}$ (h μg L^{-1})	14421.5	13786.7	9526.1	10955	13838.6
$AUC_{0-48\,h}$ (h μg L^{-1})	5134.1	5845.1	4838.3	4583.6	4491.9
V_{ss} (mL kg^{-1})	1887.0	1632.5	1737.9	2088.5	2321.7
V_{ss} (% TBW)	264	229	243	293	325
CL_B (mL h^{-1} kg^{-1})	17.3	18.1	26.2	22.8	18.1
$t_{½}$ (h)	75.8	64.4	45.9	63.2	91.6

Mean values and variances for the primary TK parameters were summarized for the low and high dose groups (Table 25).

Table 25. Kinetic parameter mean values (SD) for RBT injected with a low (44.7 μg kg^{-1}) or high (250.0 μg kg^{-1}) dose of IMI (n = 5 ea).

Parameter	Low dose	High dose
$AUC_{0-\infty}$ (h μg L^{-1})	2416.3 (851.1)	12505.6 (2142.0)
$AUC_{0-48\,h}$ (h μg L^{-1})	1095.9 (851.1)	4978.6 (544.9)
V_{ss} (mL kg^{-1})	1561.9 (65.3)	1922.5 (269.8)
V_{ss} (% TBW)	218.8 (9.10)	269.3 (37.8)
CL_B (mL h^{-1} kg^{-1})	20.5 (7.1)	20.5 (3.9)
$t_{½}$ (h)	65.6 (22.5)	68.2 (16.9)

The models assumed that elimination of IMI followed 1st order kinetics (i.e., the elimination rate was proportional to the chemical concentration). The calculated terminal elimination rate

constants (k) were 0.0117 h^{-1} (low dose) and 0.0107 h^{-1} (high dose). These rate constants correspond to terminal elimination half lives ($t_{1/2}$) of 65.6 and 68.2 h, respectively. The nominal low:high dose ratio was approximately 0.18. This was mirrored by a low:high $AUC_{0-\infty}$ ratio of 0.19. The estimated CL_B values were identical. The calculated average V_{ss} values for the low and high doses (1561.9 and 1922.5 mL kg^{-1}) were significantly different, however (unpaired, two-tailed t test using Excel, p = 0.0191). Despite the difference in V_{ss} values, the results as a whole would suggest no dose-dependence on kinetics at the administered dosing levels.

Distribution. Mean IMI residue concentrations were calculated for select low and high dose tissues at 48 h post-bolus i.a. injection. These values were then used to calculate a set of tissue:plasma concentration ratios (Table 26). The approximate LOQ and LOD, based on a 2.5x dilution during processing and reconstitution of the samples, were 2.5 and 0.8 μg kg^{-1}, respectively. The background concentrations measured in clean control tissue samples (n = 2 ea.) were as follows: 3.9 μg kg^{-1} (brain), 4.1 μg kg^{-1} (kidney), 5.7 μg kg^{-1} (liver) and 2.0 μg kg^{-1} (white muscle).

Table 26. Mean tissue IMI residue concentrations (SD) and tissue:plasma ratios from low and high dose RBT 48 h post-IMI bolus injection, n = 5 replicates except high dose brain (n = 4) and high dose white muscle (n = 3).

	Low dose		High dose	
Sample	Concentration (μg kg^{-1})	Tissue:plasma ratio	Concentration (μg kg^{-1})	Tissue:plasma ratio
Brain	19.6 (2.6)	1.4 (0.1)	98.5 (16.9)	1.3 (0.1)
Kidney	44.7 (6.0)	3.2 (0.3)	257.9 (32.3)	3.4 (0.4)
Liver	41.9 (7.9)	3.0 (0.4)	228.7 (26.4)	3.0 (0.3)
White muscle	22.4 (1.8)	1.7 (0.3)	118.8 (12.5)	1.6 (0.1)

It was assumed that internal equilibrium of the chemical was attained by the end of the distribution phase – somewhere between 8 – 12 h. By 48 h tissue:plasma ratios reflected the

relative affinity for IMI in the measured tissues under near-equilibrium conditions. Likewise, the V_{ss} can be viewed as the whole-body affinity of the fish for IMI relative to that of blood plasma. The approximate V_{ss} of 1.7 L kg^{-1} for both groups matched their 48 h white muscle:plasma ratios. White muscle, constituting approximately 50% of RBT body weight, represents a significant determinant of overall chemical affinity in the body [76, 77]. The higher tissue:plasma ratios measured in the kidney and liver was likely indicative of greater binding in these tissues and/or the activity of concentrating transporters [72].

Relatively polar compounds with a low log K_{ow} such as IMI would be predicted to distribute primarily to body water, thereby possessing a comparatively modest V_{ss}. Binding affinity for blood cells and/or tissues would result in a higher apparent V_{ss} [24, 72, 78]. RBT have a combined fraction of extra- and intra-cellular water to plasma water of approximately 0.85 [79, 80]. Assuming minimal binding to blood cells, tissue:plasma ratios of 0.85 would be indicative of equivalent distribution of IMI throughout total body water. The higher measured tissue:plasma concentration ratios suggest that IMI binds to cellular components within tissues (binding affinity for blood cells was not evaluated). Assuming equal distribution of IMI throughout total body water, the expected V_{ss} would be approximately equivalent to TBW (714 mL kg^{-1}). The greater than two-fold difference in V_{ss} over TBW provided further evidence of likely extra- or intra-cellular IMI tissue binding (along with the possibility of blood cell binding).

Elimination. The amount of IMI eliminated between 0 – 48 h was determined for all samples by calculating the product of CL_B and $AUC_{0\text{-}48\ h}$ [72]. Mean elimination values and the percent of the nominal dose eliminated for the low and high dose groups were calculated (Table 27). The average elimination at 48 h for the two dosing groups was roughly 44% of the nominal dose.

Table 27. Elimination (SD) of IMI in low and high dose fish from 0 – 48 h post-injection (n = 5 ea).

Dose group	IMI eliminated (μg kg^{-1})	Amount of nominal dose eliminated (%)	Amount of nominal dose remaining (μg kg^{-1})
Low	21.5 (4.5)	48.1 (10.1)	23.2
High	101.4 (17.6)	40.4 (7.0)	148.6

Measured IMI residue concentrations in expired branchial water were determined for both the low and high dose fish (Table 28). The approximate LOQ and LOD, based on a 400x concentration factor were 2.5 and 0.8 ng L^{-1} respectively. The mean background concentrations (SD) from branchial water samples measured pre-IMI injection were 2.9 (1.1) ng L^{-1} (low dose, n = 4), and 1.4 (0.9) ng L^{-1} (high dose, n = 5).

Table 28. Branchial water mean concentrations (SD) for RBT injected with a low (44.7 μg kg^{-1}) or high (250 μg kg^{-1}) dose of IMI.

Low dose		High dose	
Time (h)	Concentration (ng L^{-1})	Time (h)	Concentration (ng L^{-1})
1 (n = 5)	28.9 (5.0)	1 (n = 4)	230.0 (72.1)
2 (n = 5)	22.5 (7.0)	2 (n = 5)	207.8 (107.2)
4 (n = 0)	N/A	4 (n = 5)	111.7 (24.1)
8 (n = 5)	21.1 (4.3)	8 (n = 5)	97.1 (23.6)
16 (n = 3)	33.0 (2.6)	16 (n = 2)	117.5
24 (n = 5)	24.6 (7.6)	24 (n = 5)	82.3 (21.8)
36 (n = 5)	23.5 (6.5)	36 (n = 3)	57.7 (24.5)
48 (n = 4)	12.8 (3.7)	48 (n = 4)	40.4 (6.9)

Similarly to uptake, IMI present in the blood flowing through the gills would diffuse across epithelial layers. The rate of diffusion would be dependent on the difference in chemical concentration between the blood and inspired water. Branchial elimination (as determined by branchial water concentrations) would be proportional to the IMI concentration in the blood [24].

Decreases in branchial water concentrations over time would correspond with the observed decreases in plasma IMI residue concentrations.

Higher measured concentrations at several of the later depuration times were contrary to prediction. These inconsistencies may have resulted from slight differences in sample preparation. Samples were prepared in groups according to time period. Variability among samples at each time period may have been influenced by the SPE purification step during sample preparation: slight differences in processing samples could have been magnified by the 100- to 200-fold concentrations. This may have accounted for artificially high or low measured concentrations at respective time periods. Samples from time periods 1, 2, 4 and 8 h were prepared at the EPA in Duluth, MN, the remainder at the UW.

Branchial elimination profiles were developed for each high dose fish (Fig. 14). Inconsistencies in the low dose data were too great for accurate analysis. Power equations were fitted to the high dose data points and integrated from 0 – 48 h for determination of the branchial water AUC. The 0 – 48 h branchial elimination mass of IMI was determined for each sample by calculating the product of each branchial water AUC and the individually measured ventilation volume (mean = 12.9 L h^{-1}, SD = 2.9 L h^{-1}), normalized to body mass. The mean value (SD) was 57.2 (12.0) μg kg^{-1}. The high dose branchial elimination profile appeared to follow the plasma concentration-time profile depicted in Fig. 13: decreased branchial water concentrations corresponded with declines in plasma concentrations at latter time periods. A relatively strong correlation (R^2 = 0.8702) among data points was calculated for the power regression.

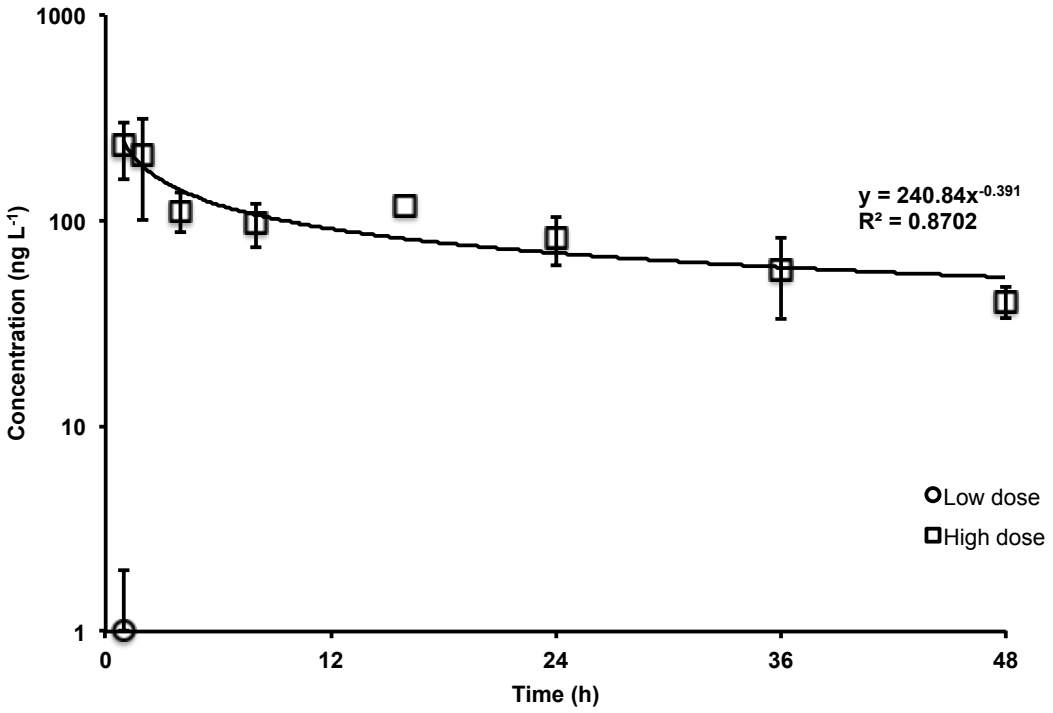

Fig. 14. Log-transformed branchial elimination profiles for the high dose RBT following bolus i.a. injections of IMI. Data points are the sample means ± SD.

Mean IMI residue concentrations (SD) in bile from the low (n = 5) and high (n = 4) dose samples at 48 h post-bolus i.a. injections were 69.3 (5.2) and 442.2 (75.4) μg L^{-1}, respectively. The approximate LOQ and LOD, based on a 2.5x dilution during processing and reconstitution of the samples, were 2.5 and 0.8 μg L^{-1}. The background concentrations measured in clean control bile samples were 1.5 and 1.1 μg L^{-1} (female and male, n = 1 ea). The 0 – 48 h biliary secretion mass of IMI was determined for each sample by calculating the product of the individually measured bile concentration at 48 h and the volume of bile collected, normalized to body mass The mean values (SD) for the low and high dose groups were 0.1 (0.1) and 1.6 (0.6) μg kg^{-1}, respectively. Unlike quantitation of excreted chemical in the feces, residues in the bile cannot be considered truly eliminated. No account was made for possible enterohepatic cycling – the release of bile from the gall bladder into the small intestine and subsequent reabsorption

into the circulation. Given the relatively small size and polarity of IMI, this component of distribution could account for a portion of the chemical that would ultimately be incorporated into the systemic circulation [72].

IMI residue concentrations were measured in urine from one low dose fish. The mass of IMI residues eliminated at each time interval was determined by calculating the product of the urine concentration and volume over the collection period. Total renal elimination of IMI from 0 – 48 h, normalized to body mass, was 6.5 μg kg^{-1}.

Clearance. Branchial clearance (CL_b), the biliary contribution to hepatic clearance ($CL_{h\text{-}bi}$) and renal clearance (CL_r) were determined for individual fish by calculating the quotient of each normalized IMI mass eliminated from 0 – 48 h over the calculated $AUC_{0\text{-}48\ h}$ [72]. The percent contribution of each to overall body clearance was also calculated (Table 29).

Table 29. Whole body, branchial, biliary and renal clearance values (percent contribution to whole body clearance) for RBT injected with a low (44.7 μg kg^{-1}) or high (250 μg kg^{-1}) dose of IMI.

Low dose			
Fish	Whole body clearance CL_B (mL h^{-1} kg^{-1})	Biliary clearance $CL_{h\text{-}bi}$ (mL h^{-1} kg^{-1})	Renal clearance CL_r (mL h^{-1} kg^{-1})
L1	19.2	0.3 (1.6%)	5.6 (29.2%)
L2	28.4	0.4 (1.4%)	N/A
L3	12.7	0.3 (2.4%)	N/A
L4	14.8	0.4 (2.7%)	N/A
L5	27.2	0.4 (1.5%)	N/A
High dose			
Fish	Whole body clearance CL_B (mL h^{-1} kg^{-1})	Branchial clearance CL_b (mL h^{-1} kg^{-1})	Biliary clearance $CL_{h\text{-}bi}$ (mL h^{-1} kg^{-1})
H1	17.3	9.8 (56.7%)	0.6 (3.5%)
H2	18.1	7.2 (39.8%)	0.8 (4.4%)
H3	26.2	9.1 (34.7%)	0.5 (1.9%)
H4	22.8	11.2 (49.1%)	N/A
H5	18.1	11.4 (63.0%)	0.6 (3.3%)

Mean clearance values and variances were summarized using data for both the low and high dose groups (Table 30). Branchial, biliary and renal clearance percent contributions to overall clearance were calculated for the low and high dose groups (Table 31). The combined contributions to overall clearance were approximately 77%. Expectations for high branchial clearance given the physicochemical characteristics of IMI were confirmed: branchial clearance accounted for almost 50% of the total body clearance. Although based on data from only one low dose sample, expectations for high renal clearance as reported in mammals were likewise realized [28]. The efficiency of the alternative branchial clearance pathway could account for the lower overall contribution of renal clearance in RBT relative to mice.

Table 30. Mean whole body, branchial, biliary and renal clearance values (SD) for RBT injected with a low (44.7 µg kg^{-1}) or high (250 µg kg^{-1}) dose of IMI.

Dose group	Whole body clearance CL_B (mL h^{-1} kg^{-1})	Branchial clearance CL_b (mL h^{-1} kg^{-1})	Biliary clearance $CL_{h\text{-}bi}$ (mL h^{-1} kg^{-1})	Renal clearance CL_r (mL h^{-1} kg^{-1})
Low	20.5 (7.1)	N/A	0.1 (0.0)	5.6
High	20.5 (3.9)	9.7 (1.7)	0.4 (0.2)	N/A

Table 31. Branchial, biliary and renal clearance percent contributions to overall clearance based on low or high dose whole body clearances.

CL_b (high dose, n = 5)	$CL_{h\text{-}bi}$ (low dose, n = 5)	$CL_{h\text{-}bi}$ (high dose, n = 4)	CL_r (low dose, n = 1)
47.3	< 0.1	1.9	27.3

As discussed above, the biliary secretion of chemical should not be equated with elimination. The actual biliary contribution to hepatic and whole body clearance may be lower than calculated for the low and high dose groups. In either case, the measured biliary clearance values were

minor, amounting to less than 2% of overall clearance. The effect from considerable enterohepatic cycling would be a further reduction of their significance.

9. Hepatic metabolism study

Due to errors with sample preparation, only one set of 1.0 μM active and denatured fractions was successfully quantitated. The LOQ and LOD could not be determined, however. No loss of substrate was observed over the 2-h incubation period in either the active or denatured liver S9.

Studies using recombinant human liver CYPs identified the isozymes selective for oxidation (CYP3A4, CYP2C19, CYP2A6 and CYP2C9) and reduction (CYP1A2, CYP2B6, CYP2D6 and CYP2E1) of either the imidozolidine or nitrosoimine IMI moieties [34]. RBT possess two of these CYP isozymes: CYP1A and CYP3A45 [81]. The RBT CYP1A is not orthologuous to the human 1A2, however [82]. The limited homology to its human counterpart may result in little to no metabolic activity. CYP3A45 is mainly expressed in the GIT, minimizing its potential metabolic activity in the liver [83]. Nitrosoimine reduction by cytosolic aldehyde oxidase (AOX) was measured in mammals and birds [32, 33]. Metabolic rates differed widely among species, with some measurement barely above background [32]. Likewise, RBT AOX reducing activity may be very low.

Although the S9 preparations allowed for investigation of microsomal (CYP) and cytosolic (AOX) enzyme activity, a more sensitive assay may have been required for defining RBT hepatic metabolism of IMI. The results from the present S9 study indicate that metabolic elimination may not make a significant contribution to overall removal of IMI. The physicochemical characteristic of the compound – small, un-ionized, relatively polar – may favor biliary secretion of the compound unchanged as the primary route of removal from the liver [72].

Calculations discussed previously indicate that biliary clearance of IMI is not a significant contributor to overall clearance, however.

RBT/white sturgeon comparisons

Measured tissue:plasma IMI residue concentration ratios in RBT (Table 26) were slightly higher than those of white sturgeon (Table 21). Under the assumption that internal chemical equilibrium was achieved by the time of measurement, the differing ratios could be the result of species-specific differences in binding. Although limited, the data suggest that both species handle the chemical in a similar manner.

Effects characterization

The only assessment endpoint investigated in the current study was the 96-h median lethal toxicity (LC_{50}) in FW juvenile white sturgeon. Sublethal effects – physiological and behavioral impacts that may impair the fish, potentially reducing overall fitness and imperiling survival – were not examined. One such endpoint commonly observed in acute lethal toxicity exposures is lethargy, defined as a diminished or non-response to outward stimuli. Due to the inherent tranquil disposition of white sturgeon, it was not possible to ascertain such an effect. Lethargy was observed in an unpublished, comparable 96-h acute IMI exposure with SW adapted juvenile Chinook, however. The LC_{50} for juvenile Chinook was 109 mg L^{-1}. At the end of 96 h, lethargy was observed in all of the fish exposed to IMI at a concentration of 66 mg L^{-1}. No lethargy was observed in fish at the lowest test concentration (46 mg L^{-1}). Assuming comparable behavior in sturgeon, the onset and extent of the lethargic response would occur in a narrow concentration band only slightly below the median lethal toxicity.

Outcomes such as lethargy and lethality in green sturgeon would be unlikely in the field: worst-case pore water IMI residue concentrations were predicted to be approximately 3 orders of magnitude lower and durations of exposure $1/24^{th}$ of those used for development of the LC_{50}. No effects were observed in the simulated field exposures with SW-adapted white sturgeon. These tests were conducted at comparable concentrations and time durations as determined in the exposure characterization.

The potential for toxic effects occurring under long-term exposure conditions were also examined. Acute-chronic ratios (ACRs) were developed for two species for use in predicting chronic effects in green sturgeon [84]. The ratio of acute (LC_{50} from a 96-h median lethal toxicity test) to chronic (no observed adverse effects concentration – NOAEC – from an early life stage test) values was calculated for RBT and Sheepshead Minnow (*Cyprinodon variegatus*). The ACR for RBT was derived from published studies [13, 85]. The acute LC_{50} of 211 mg L^{-1} and chronic NOAEC from a 36-d early life stage test of 1.2 mg L^{-1} yielded a ratio of 176. The Sheepshead Minnow ACR was developed using data from unpublished studies by C.E. Grue at co-workers at the UW. The acute LC_{50} of 60.6 mg L^{-1} and chronic NOAEC from a 32-d early life stage test of > 10 mg L^{-1} yielded a ratio of 6.1.

The greater ACR from RBT was applied to the measured acute toxicity value for white sturgeon (LC_{50} = 124 mg L^{-1}) for a predicted NOAEC of 0.7 mg L^{-1}. The value of the estimated NOAEC for green sturgeon is approximately 2 orders of magnitude greater than the highest calculated pore water concentrations (27.8 μg L^{-1}). This would indicate that overt adverse effects occurring due to chronic exposure to IMI are highly unlikely.

Exposure to IMI in green sturgeon may induce less observable sublethal effects. Although no investigations have been conducted with vertebrates, studies have suggested IMI-induced

impairment of olfaction in honeybees (*Apis mellifera*) [86]. Diminished feeding activity was measured in coho salmon (*O. kisutch*) following environmentally relevant exposures to the organophosphate (OP) insecticide chlorpyrifos [87]. This behavior was linked to toxicant-induced disruption of olfaction, reducing the ability of the fish to locate their prey. OP along with carbamate insecticides, are neurotoxicants that inhibit AChE [88]. This inhibition results in reduced response to olfactory stimuli by the olfactory sensory neurons [89]. Other toxicants, such as metals and herbicides, possess different mechanisms of olfactory toxicity [89]. The ACh-agonist IMI could also disrupt olfactory response.

A literature review was conducted for investigation of other toxicity endpoints associated with exposure to IMI. IMI has been classified as non-carcinogenic in humans [29, 90]. Reproductive and teratogenic effects were observed in rats and rabbits – but at levels of exposure that were toxic to the parents [29, 30, 91]. Although no studies in fish were identified, the relatively low concentrations and ephemeral nature of the exposures in the field along with their timing and location relative to spawning marginalize these concerns. No data were found on the potential for IMI to disrupt endocrine function. IMI was initially included in the USEPA Endocrine Disruptor Screening Program (EDSP), but was omitted from the draft second list of chemicals for Tier I screening [92].

Even if a sublethal effect were detected, such an effect would have to be linked to evidence that it would lower an individual's fitness, as measured by the impact of the effect on survival, growth, or reproduction. Supporting studies would have to be conducted to provide proof of the relationship between the effect and a decrease in fitness [2]. This would require quantifying the effect on green sturgeon exposed to IMI in Willapa Bay, taking into account variables such as the size and maturity of the fish, and the physical distance and timing of the exposures relative to

spawning events. As previously noted, no overt sublethal effects have been observed in laboratory studies with SW-adapted white sturgeon at environmentally relevant concentrations.

Hazard quotient

The acute toxicity effects data and exposure characterization discussed above were incorporated into a concentration-ratio hazard quotient (HQ) for an evaluation of the likelihood of adverse effects from IMI exposure to green sturgeon in Willapa Bay [24, 29, 93, 94]. The HQ value defines the hazard associated with exposure to IMI (i.e., the ability of the chemical to cause adverse effects). The concentration-ratio approach was designed to avoid the likelihood of making decisions resulting in a false negative (Type II error). The magnitude of the HQ value would be suggestive of potential effects – or absence thereof – from exposure. This was calculated as the ratio of predicted exposure over toxicity: the estimated worst-case pore water field exposure concentration (justified because branchial uptake from pore water would account for most of the systemic absorption) was divided by the juvenile white sturgeon 96-h median lethal toxicity value.

The white sturgeon 96-h LC_{50} was 124 mg L^{-1}. The worst-case field exposure was estimated to occur at the first high tide post-IMI application. IMI exposure concentration was assumed to be 27.8 μg L^{-1}.

Despite dilution from the overlying water, the decrease in pore water concentrations over successive tidal cycles, along with intermittent recovery periods off of the beds during low tides, the 27.8 μg L^{-1} exposure concentration was assumed to be continuous for the 96-h period. The HQ was calculated as follows:

$$HQ = \frac{\text{Exposure estimate}}{\text{Effect benchmark}} = \frac{27.8\ \mu g\ L^{-1}}{124{,}000\ \mu g\ L^{-1}} = \mathbf{0.0002}$$

The calculated HQ was compared to the USEPA level of concern (LOC) for direct effects from acute exposure to endangered species [94]. The results were two orders of magnitude below the 0.05 threshold that USEPA uses for evaluating the potential likelihood of effects. Comparable HQ values for IMI were previously reported for RBT (0.00008) and Sheepshead Minnow (0.00011) [95]. Considering the extreme magnitude of the IMI concentration and the inflated duration of the exposure incorporated into the green sturgeon estimate, the likelihood of adverse effects to green sturgeon from exposure to IMI in Willapa Bay suggested by the HQ is extremely low. Furthermore, the large distance in the point value of the HQ from the level of concern obviates uncertainty based on species or individual sensitivities.

The value of the derived HQ provides a large safety margin between the calculated worst-case exposure and the measured adverse effect concentration for lethality. While the likelihood of effects from an acute exposure is extremely small, this approach does not account for potential sublethal effects that may result from exposures at or below the worst-case level [2]. Nor does it recognize the potential for effects from repeated annual short-term exposures. Additionally, it does not impart insight into the probability of any adverse effects and is therefore not a measure of risk [2].

A probabilistic approach would define the mathematical likelihood for adverse effects. Such an approach would incorporate uncertainties in the exposure and effects characterizations – the frequency of use and amount of time sturgeon forage on the beds, all activities that could lead to IMI exposure, and all potential adverse effects – into probability distributions. The likelihood of adverse effects would be provided over a range of exposures [2].

Given the results of the exposure characterization – and their wide disparity from conditions necessary for inducing observed adverse effects – a probabilistic approach may not be warranted. Although uncertainty exists in the exposure and effects characterization, the evidence suggests minimal risk to green sturgeon from exposure to IMI following applications in Willapa Bay.

Summary

The primary goals of this study were to determine the potential for green sturgeon to be exposed to IMI, characterize the environmental exposure, and describe the disposition of the chemical following uptake. Achievement of these goals necessitated quantification of IMI residues in multiple sample matrices. Sample preparation and LC-MS/MS detection protocols were optimized and validated across sample mediums, prior to utilization in the study. IMI was applied to test beds in Willapa Bay. Preferential feeding by green sturgeon on IMI-impaired burrowing shrimp was confirmed following application of the chemical on the beds. Pore water and burrowing shrimp were identified as the main sources of IMI exposure to green sturgeon. Exposure was characterized in the two mediums. Worst-case IMI exposures over the 4-h foraging time window of the high tide cycle immediately following IMI application were modeled by incorporating data from the pore water and burrowing shrimp exposure characterizations resulting in estimations of branchial and dietary uptake of 177.9 and 3.8 μg per kg body weight, respectively.

Juvenile white sturgeon were used as surrogates for green sturgeon in controlled acute exposure studies. The 96-h median lethal toxicity was 124 mg L^{-1}. Mean plasma IMI residue concentrations in white sturgeon following modeled worst-case water exposures over three successive tidal cycles were 11.8, 8.2 and 8.6 μg kg^{-1}. These concentrations would represent the

expected ceiling for plasma concentrations measured in green sturgeon during environmental monitoring following operational applications of IMI in Willapa Bay. Plasma residues were quantitated in 20 green sturgeon collected approximately 30 h post-IMI application on the test beds. No IMI residues were detected.

Kinetic parameters were determined in RBT injected with a low (44.7 μg kg^{-1}) or high (250.0 μg kg^{-1}) dose of IMI. Mean values were: V_{ss} (1561.9, 1922.5 mL kg^{-1}), CL_B (20.5 mL h^{-1} kg^{-1}) and $t_{1/2}$ (65.6, 68.2 h) for the low and high dose groups, respectively.

Conclusion

Although a seasonal green sturgeon population estimate is currently being developed, it is suspected that as many as 2000 green sturgeon could occupy Willapa Bay during the chemical applications in July (O. Langness, Washington Department of Fish and Wildlife, Vancouver, WA, personal communication). The number of green sturgeon caught in the environmental monitoring effort following the experimental test bed applications was small relative to the overall population. Additionally, acoustic telemetry readings of 'tagged' green sturgeon indicate they move extensively throughout the Bay [20]. The small sample size, coupled with movement out of the area, likely reduced the chance of capturing an IMI-exposed fish. The absence of positive detects (i.e., quantified residues in plasma) from the subset of fish sampled, does not imply that other green sturgeon were not exposed.

Annual operational IMI applications would cover an area approximately 16-fold greater than that in the present study. The intertidal mudflats in Willapa Bay comprise an area of 17,200 ha, of which ca. 3642 ha (21%) are cultivated oyster beds [8]. IMI applications would be limited to approximately 240 ha per year; an area comprising 1.4% of the total intertidal mudflats (K

Patten, Washington State University, Long Beach, WA, personal communication). Applications would take place over two successive tidal cycles each July, typically 2-weeks apart, with beds receiving re-treatment on a 3-year rotation.

The greater use of IMI spread across multiple regions of Willapa Bay, coupled with the extended application time window, would increase the likelihood for chemical exposure to green sturgeon. Even under worst-case exposure scenarios, IMI uptake in sturgeon via water and food was shown to be modest. Concentrations were two and three orders of magnitude lower than those predicted to elicit acute or chronic effects, respectively. The chemical appears to behave similarly in both RBT and sturgeon: once taken up, IMI is moderately persistent in either species. The length of the elimination half-life provides a window of opportunity for environmental monitoring. This may be warranted to confirm that exposures do not exceed those predicted in the present study.

This study was intended as an assessment of environmental and systemic exposure to IMI in green sturgeon. Analysis of the data developed in these investigations was used to model worst-case IMI exposure scenarios for green sturgeon and provide insight into the persistence of the chemical in the fish. The risk characterization was weighted heavily by the results of the exposure assessment. Data are lacking for sublethal effects associated with IMI exposure. Despite the scarcity of effects information, green sturgeon are expected to be at minimal risk from exposure to IMI in Willapa Bay.

REFERENCES

1. National Marine Fisheries Service. 2010. Environmental Assessment for the Proposed Application of Protective Regulations Under Section 4(D) of the Endangered Species Act for the Threatened Southern Distinct Population Segment of North American Green Sturgeon. Green Sturgeon Final 4(d) rule, Final NEPA EA. U.S. Department of Commerce, Washington DC.
2. National Research Council of the National Academies. 2013. Assessing Risks to Endangered and Threatened Species from Pesticides. National Academy of Sciences, Washington, D.C.
3. Moyle PB. 2002. *Inland fishes of California*. University of California Press, Berkeley, CA.
4. Adams PB, Grimes C, Hightower JE, Lindley ST, Moser ML, Parsley MJ. 2007. Population status of North American green sturgeon, *Acipenser medirostris*. *Environmental Biology of Fishes 79*:339-356.
5. Israel JA, May B. 2007. Mixed Stock Analysis of Green Sturgeon from Washington State Coastal Aggregations. University of California, Davis, CA.
6. National Marine Fisheries Service. 2006. Endangered and Threatened Wildlife and Plants: Threatened Status for Southern Distinct Population Segment of North American Green Sturgeon. Federal Register 71:67. U.S. Department of Commerce, Washington, DC.
7. National Marine Fisheries Service. 2009. Endangered and Threatened Wildlife and Plants: Final Rulemaking to Designate Critical Habitat for the Threatened Southern Distinct Population Segment of North American Green Sturgeon; Final Rule. Federal Register 74:195. U.S. Department of Commerce, Washington, DC.
8. Feldman KL, Armstrong DA, Dumbauld BR, DeWitt TH, Doty DC. 2000. Oysters, crabs, and burrowing shrimp: Review of an environmental conflict over aquatic resources and pesticide use in Washington State's (USA) coastal estuaries. *Estuaries* 23:141-176.
9. Dumbauld BR, Brooks KM, Posey MH. 2001. Response of an estuarine benthic community to application of the pesticide carbaryl and cultivation of Pacific oysters (*Crassostrea gigas*) in Willapa Bay, Washington. *Marine Pollution Bulletin* 42:826-844.
10. Labenia JS, Baldwin DH, French BL, Davis JW, Scholz NL. 2007. Behavioral impairment and increased predation mortality in cutthroat trout exposed to carbaryl. *Marine Ecology-Progress Series 329*:1-11.
11. Felsot AS, Ruppert JR. 2002. Imidacloprid residues in Willapa Bay (Washington State) water and sediment following application for control of burrowing shrimp. *Journal of Agricultural and Food Chemistry* 50: 4417-4423.
12. Matsuda K, Buckingham SD, Kleier D, Rauh JJ, Grauso M, Sattelle DB. 2001. Neonicotinoids: insecticides acting on insect nicotinic acetylcholine receptors. *Trends in Pharmacological Sciences* 22:573-580.
13. Grau, R. 1988. Leverkusen-Bayerwerk Report No. 101303. Bayer AG, Leverkusen, North Rhine-Westphalia, Germany.
14. Hartley D, Kidd H. 1991. *The agrochemicals handbook. 3rd ed.* Royal Society of Chemistry, Cambridge, England.
15. Buckingham SD, Lapied B, LeCorronc H, Grolleau F, Sattelle DB. 1997. Imidacloprid actions on insect neuronal acetylcholine receptors. *Journal of Experimental Biology* 200:2685-2692.
16. Tomizawa M, Casida JE. 2003. Selective toxicity of neonicotinoids attributable to specificity of insect and mammalian nicotinic receptors. *Annual Review of Entomology* 48:339-364.
17. Honda H, Tomizawa M, Casida JE. 2006. Insect nicotinic acetylcholine receptors: Neonicotinoid binding site specificity is usually but not always conserved with varied substituents and species. *Journal of Agricultural and Food Chemistry* 54:3365-3371.
18. Hellpointner JK. 2002. Environmental fate of imidacloprid. Bayer AG, Leverkusen, North Rhine-Westphalia, Germany.
19. Rosenfeldt F. 1992. Dissociation Constant of NTN 33893, Report No. PC317. Bayer AG, Leverkusen, North Rhine-Westphalia, Germany.
20. Moser ML, Lindley ST. 2007. Use of Washington estuaries by subadult and adult green sturgeon. *Environmental Biology of Fishes* 79:243-253.
21. Dumbauld BR, Holden DL, Langness OP. 2008. Do sturgeon limit burrowing shrimp populations in Pacific Northwest Estuaries? *Environmental Biology of Fishes* 83:283-296.
22. LeBreton GTO, Beamish FWH, McKinley RS. 2004. *Sturgeons and paddlefish of North America*. Kluwer Academic Publishers, Boston, MA.

23. McKim J, Schmieder P, Veith G. 1985. Absorption dynamics of organic-chemical transport across trout gills as related to octanol water partition-coefficient. *Toxicology and Applied Pharmacology* 77:1-10.
24. Di Giulio RT, Hinton DE. 2008. *The toxicology of fishes*. Boca Raton, FL.
25. McKim JM, Nichols JW, Lien GJ, Hoffman AD, Gallinat CA, Stokes GN. 1996. Dermal absorption of three waterborne chloroethanes in rainbow trout (*Oncorhynchus mykiss*) and channel catfish (*Ictalurus punctatus*). *Fundamental and Applied Toxicology* 31:218-228.
26. Arnot JA, Gobas FA. 2006. Review of bioconcentration factor (BCF) and bioaccumulation factor (BAF) assessments for organic chemicals in aquatic organisms. *Environmental Reviews* 14:257-297.
27. Costanza J, Lynch DG, Boethling RS, Arnot JA. 2012. Use of the bioaccumulation factor to screen chemicals for bioaccumulation potential. *Environmental Toxicology and Chemistry* 31:2261-2268.
28. Ford KA, Casida JE. 2006. Chloropyridinyl neonicotinoid insecticides: Diverse molecular substituents contribute to facile metabolism in mice. *Chemical Research in Toxicology* 19:944-951.
29. National Pesticide Information Center. Imidacloprid Technical Fact Sheet. Oregon State University, Corvalis, OR.
30. Solecki R. 2001. Toxicological evaluations: Imidacloprid. INCHEM, Federal Institute for Health Protection of Consumers Veterinary Medicine, Berlin, Germany.
31. Casida JE. 2011. Neonicotinoid metabolism: Compounds, substituents, pathways, enzymes, organisms, and relevance. *Journal of Agricultural and Food Chemistry* 59:2923-2931.
32. Dick RA, Kanne DB, Casida JE. 2005. Identification of aldehyde oxidase as the neonicotinoid nitroreductase. *Chemical Research in Toxicology* 18:317-323.
33. Honda H, Tomizawa M, Casida JE. 2006. Neonicotinoid metabolic activation and inactivation established with coupled nicotinic receptor-CYP3A4 and -aldehyde oxidase systems. *Toxicology Letters* 161:108-114.
34. Schulz-Jander DA, Casida JE. 2002. Imidacloprid insecticide metabolism: Human cytochrome P450 isozymes differ in selectivity for imidazolidine oxidation versus nitroimine reduction. *Toxicology Letters* 132:65-70.
35. Schulz-Jander DA, Leimkuehler WM, Casida JE. 2002. Neonicotinoid insecticides: Reduction and cleavage of imidacloprid nitroimine substituent by liver microsomal and cytosolic enzymes. *Chemical Research in Toxicology* 15:1158-1165.
36. Schoning R, Schmuck R. 2003. Analytical determination of imidacloprid and relevant metabolite residues by LC MS/MS. *Bulletin of Insectology* 56:41-50.
37. Wegscheider W. 1996. Validation of analytical methods. In Guenzler H, ed, *Accreditation and quality assurance in analytical chemistry.* Springer Verlag, Berlin, Germany, pp 135-158.
38. EnviroLogix. 2011. QuantiPlate™ Kit for Imidacloprid. Portland, ME. [cited 15 January 2013]. Available from: http://www.envirologix.com/artman/publish/article_72.shtml
39. Ohno I, Tomizawa M, Durkin KA, Naruse Y, Casida JE, Kagabu S. 2009. Molecular features of neonicotinoid pharmacophore variants interacting with the insect nicotinic receptor. *Chemical Research in Toxicology* 22:476-482.
40. Tomizawa M, Zhang NJ, Durkin KA, Olmstead MM, Casida JE. 2003. The neonicotinoid electronegative pharmacophore plays the crucial role in the high affinity and selectivity for the *Drosophila* nicotinic receptor: An anomaly for the nicotinoid cation-pi interaction model. *Biochemistry* 42:7819-7827.
41. Kagabu S, Ishihara R, Hieda Y, Nishimura K, Naruse Y. 2007. Insecticidal and neuroblocking potencies of variants of the imidazolidine moiety of imidacloprid-related neonicotinoids and the relationship to partition coefficient and charge density on the pharmacophore. *Journal of Agricultural and Food Chemistry* 55:812-818.
42. Tomizawa M, Lee DL, Casida JE. 2000. Neonicotinoid insecticides: Molecular features conferring selectivity for insect versus mammalian nicotinic receptors. *Journal of Agricultural and Food Chemistry* 48:6016-6024.
43. Kanne DB, Dick RA, Tomizawa M, Casida JE. 2005. Neonicotinoid nitroguanidine insecticide metabolites: Synthesis and nicotinic receptor potency of guanidines, aminoguanidines, and their derivatives. *Chemical Research in Toxicology* 18:1479-1484.
44. Liu WP, Zheng W, Ma Y, Liu KK. 2006. Sorption and degradation of imidacloprid in soil and water. *Journal of Environmental Science and Health, Part B. Pesticides Food Contaminants and Agricultural Wastes* 41:623-634.
45. Wamhoff H, Schneider V. 1999. Photodegradation of imidacloprid. *Journal of Agricultural and Food Chemistry* 47:1730-1734.

46. Fossen, M. 2006. Environmental fate of imidacloprid. California Department of Pesticide Regulation, Sacramento, CA.
47. Chao SL, Casida JE. 1997. Interaction of imidacloprid metabolites and analogs with the nicotinic acetylcholine receptor of mouse brain in relation to toxicity. *Pesticide Biochemistry and Physiology* 58:77-88.
48. Nauen R, Ebbinghaus-Kintscher U, Schmuck R. 2001. Toxicity and nicotinic acetylcholine receptor interaction of imidacloprid and its metabolites in *Apis mellifera* (Hymenoptera : Apidae). *Pest Management Science* 57:577-586.
49. U.S. Environmental Protection Agency. 1993. Hazardous Waste Management System; Testing and Monitoring Activities. Federal Register. 58:167. U.S. Environmental Protection Agency, Washington, D.C.
50. Zheng W, Liu WP. 1999. Kinetics and mechanism of the hydrolysis of imidacloprid. *Pesticide Science* 55:482-485.
51. Erickson RJ, McKim JM. 1990. A simple flow-limited model for exchange of organic-chemicals at fish gills. *Environmental Toxicology and Chemistry* 9:159-165.
52. Gobas F, Muir DC, Mackay D. 1988. Dynamics of dietary bioaccumulation and fecal elimination of hydrophobic organic-chemicals in fish. *Chemosphere* 17:943-962.
53. Spokane Tribe of Indians. 2013. Lake Roosevelt White Sturgeon Recovery Project. Willpinit, WA [cited 20 June 2013]. Available from: http://www.spokanetribe.com/dnr-sturgeon-recovery
54. Ecological Effects Test Guidelines. 1996. OPPTS 850.1075 Fish Acute Toxicity Test, Freshwater and Marine. EPA 712-C-96-118. U.S. Environmental Protection Agency, Washington, DC.
55. Frew JA, Grue CE. 2012. Development of a new method for the determination of residues of the neonicotinoid insecticide imidacloprid in juvenile chinook (*Oncorhynchus tshawytscha*) using ELISA detection. *Journal of Environmental Monitoring* 14:1024-1034.
56. McEnroe M, Cech JJ. 1985. Osmoregulation in juvenile and adult white sturgeon, *Acipenser transmontanus*. *Environmental Biology of Fishes* 14:23-30.
57. Wolf K. 1986. Citation-classic - physiological salines for fresh-water teleosts. *Current Contents/Agriculture Biology and Environmental Sciences* 46:20.
58. McKim JM, Goeden HM. 1982. A direct measure of the uptake efficiecy of a xenobiotic chemical across the gills of brook trout (*Salvelinus fontinalis*) under normoxic and hypoxic conditions. *Comparative Biochemistry and Physiology Part C: Comparative Pharmacology* 72:65-74.
59. Carlson RW, Lien GW, Holmen BA. 1989. An Automated Monitoring System for Fish Physiology and Toxicology. U.S. Environmental Protection Agency, Environmental Research Laboratory, Duluth, MN.
60. Han X, Nabb DL, Yang CH, Snajdr SI, Mingoia RT. 2009. Liver microsomes and S9 from rainbow trout (*Oncorhynchus mykiss*): Comparison of basal-level enzyme activities with rat and determination of xeonbiotic intrinsic clearance in support of bioaccumulation assessment. *Environmental Toxicology and Chemistry* 28:481-488.
61. Johanning K, Hancock G, Escher B, Adekola A, Bernhard M J, Cowan-Ellsberry C, Domoradzki J, Dyer S, Eickhoff C, Embry M, Erhardt S, Fitzsimmons P, Halder M, Hill J, Holden D, Johnson R, Rutishauser S, Segner H, Schultz I, Nichols, J. 2012. Assessment of metabolic stability using the rainbow trout (*Oncorhynchus mykiss*) liver S9 fraction. *Current Protocols in Toxicology* 10:1-28.
62. Ihara M, Matsuda K, Otake M, Kuwamura M, Shimomura M, Komai K, Akamatsu M, Raymond V, Sattelle DB. 2003. Diverse actions of neonicotinoids on chicken alpha 7, alpha 4 beta 2 and *Drosophila*-chicken SAD beta 2 and ALS beta 2 hybrid nicotinic acetylcholine receptors expressed in *Xenopus laevis* oocytes. *Neuropharmacology* 45:133-144.
63. Stryer, L. 1995. *Biochemistry*. 4th ed. W.H. Freeman and Company, New York, NY.
64. Emerson K, Russo RC, Lund RE, Thurston RV. 1975. Aqueous ammonia equilibrium calculations - effect of pH and temperature. *Journal of the Fisheries Research Board of Canada* 32:2379-2383.
65. Thurston RV, Russo RC, Vinogradov GA. 1981. Ammonia toxicity to fishes - effect of pH on the toxicity of the un-ionized ammonia species. *Environmental Science and Technology* 15:837-840.
66. Cui Y, Hung SSO, Zhu, X. 1996. Effect of ration and body size on the energy budget of juvenile white sturgeon. *Journal of Fish Biology* 49:863-876.
67. Evans DH, Claiborne JB. 2006. *The physiology of fishes*. 3rd ed. CRC Taylor & Francis, Boca Raton, FL.
68. Dumbauld BR, Booth S, Cheney D, Suhrbier A, Beltran H. 2006 An integrated pest management program for burrowing shrimp control in oyster aquaculture. *Aquaculture* 261:976-992.

69. Dumbauld BR, Armstrong DA, Feldman KL. 1996. Life-history characteristics of two sympatric thalassinidean shrimps, *Neotrypaea californiensis* and *Upogebia pugettensis*, with implications for oyster culture. *Journal of Crustacean Biology* 16:689-708.
70. Erickson RJ, McKim JM. 1990. A model for exchange of organic-chemicals at fish gills - flow and diffusion limitations. *Aquatic Toxicology* 18:175-197.
71. Hayton WL, Barron MG. 1990. Rate-limiting barriers to xenobiotic uptake by the gill. *Environmental Toxicology and Chemistry* 9:151-157.
72. Rowland M, Tozer TN. 1995. *Clinical pharmacokinetics : Concepts and applications*. 3rd ed. Williams & Wilkins, Baltimore, MD.
73. PALL Medical. 2010. Plasma Optimization Guide. Improving Plasma Yields from Whole Blood Donations. Port Washington, NY: Pall Corporation. [cited 10 July 2013]. Available from: http://www.pall.com/pdfs/Medical/10.3422_Plasma_OG(1).pdf
74. Nichols DJ. 1987. Fluid volumes in rainbow trout, *Salmo gairdneri* - application of compartmental analysis. *Comparative Biochemistry and Physiology Part A: Physiology* 87:703-709.
75. Thorson TB. 1961. Partitioning of body water in osteichthyes - phylogenetic and ecological implications in aquatic vertebrates. *Biological Bulletin* 120:238.
76. Webb PW, Johnsrude CL. 1988. The effect of size on the mechanical properties of the myotomal-skeletal system of rainbow trout (*Salmo-gairdneri*). *Fish Physiology and Biochemistry* 5:163-171.
77. Goolish EM. 1989. The scaling of aerobic and anaerobic muscle power in rainbow trout (*Salmo gairdneri*). *Journal of Experimental Biology* 147:493-505.
78. Bertelsen SL, Hoffman AD, Gallinat CA, Elonen CM, Nichols JW. 1998. Evaluation of log Kow and tissue lipid content as predictors of chemical partitioning to fish tissues. *Environmental Toxicology and Chemistry* 17:1447-1455.
79. Nichols JW, McKim JM, Lien GJ, Hoffman AD, Bertelsen SL. 1991. Physiologically based toxicokinetic modeling of 3 waterborne chloroethanes in rainbow trout (*Oncorhynchus mykiss*). *Toxicology and Applied Pharmacology* 110:374-389.
80. Fitzsimmons PN, Hoffman AD, Lien GJ, Hammermeister DE, Nichols JW. 2009. Kinetics and effects of dichloroacetic acid in rainbow trout. *Aquatic Toxicology* 94:186-194.
81. Uno T, Ishizuka M, Itakura T. 2012. Cytochrome P450 (CYP) in fish. *Environmental Toxicology and Pharmacology* 34:1-13.
82. Stegeman JJ. 1994. Biochemistry and molecular biology of monooxygenases: Current perspectives on forms, functions, and regulation of cytochrome P450 in aquatic species. In Malin DC, Ostrander GR, eds, *Aquatic toxicology: molecular, biochemical, and cellular perspectives*. Lewis Publishers. Boca Raton, FL, pp 87-206.
83. Lee SJ, Buhler DR. 2003. Cloning, tissue distribution, and functional studies of a new cytochrome P450 3A subfamily member, CYP3A45, from rainbow trout (*Oncorhynchus mykiss*) intestinal ceca. *Archives of Biochemistry and Biophysics* 412:77-89.
84. Hoff D, Lehmann W, Pease A, Raimondo S, Russom C, Steeger T. 2010. Predicting the Toxicities of Chemicals to Aquatic Animal Species. U.S. Environmental Protection Agency, Washington, D.C.
85. Anatra-Cordone M, Durkin P. 2005. Imidacloprid Human Health and Ecological Risk Assessment - Final Report. U.S. Department of Agriculture, Arlington, VA.
86. Decourtye A, Armengaud C, Renou M, Devillers J, Cluzeau S, Gauthier M, Pham-Delegue MH. 2004. Imidacloprid impairs memory and brain metabolism in the honeybee (*Apis mellifera* L.). *Pesticide Biochemistry and Physiology* 78:83-92.
87. Sandahl JF, Baldwin DH, Jenkins JJ, Scholz NL. 2005. Comparative thresholds for acetylcholinesterase inhibition and behavioral impairment in coho salmon exposed to chlorpyrifos. *Environmental Toxicology and Chemistry* 24:136-145.
88. Savolainen K. 2001. Understanding the toxic actions of organophosphates. In Krieger RI, Krieger WC, eds, *Handbook of pesticide toxicology,* 2nd ed, Vol. 2. Acedemic Press, San Diego, CA, pp 1013-1042.
89. Tierney KB, Baldwin DH, Hara TJ, Ross PS, Scholz NL, Kennedy CJ. 2010. Olfactory toxicity in fishes. *Aquatic Toxicology* 96:2-26.
90. U.S. Environmental Protection Agency Office of Pesticide Programs. 2012. Chemicals Evaluated for Carcinogenic Potential. Washington, D.C. U.S. Environmental Protection Agency. [cited 25 June 2013]. Available from: http://npic.orst.edu/chemicals_evaluated.pdf
91. Thyssen J, Machemer L. 1999. Toxicology and metabolism. In Yamamoto I, Casida J, eds, *Nicotinoid insecticides and the nicotinic acetylcholine receptor*. Springer-Verlag, Tokyo, Japan, pp 213-222.

92. U.S. Environmental Protection Agency Endocrine Disruptor Screening Program (EDSP). 2013. Revised Second List of Chemicals for Tier 1 Screening. Washington, D.C.: U.S. Environmental Protection Agency. [cited 30 June 2013]. Available from: http://www.epa.gov/endo/pubs/prioritysetting/revlist2.htm
93. U.S. Envrionmental Protection Agency Science Policy Council. 2000. Risk Characterization Handbook. EPA-100-B-00-002. U.S. Environmental Protection Agency, Washington, D.C.
94. U.S. Environmental Protection Agency Office of Pesticide Programs. 2004. Overview of the Ecological Risk Assessment Process in the Office of Pesticide Programs, U.S. Environmental Protection Agency. Endangered and Threatened Species Effects Determinations. Washington, D.C.: U.S. Environmental Protection Agency. [cited 1 July 2013]. Available from: http://www.epa.gov/espp/consultation/ecorisk-overview.pdf
95. Felsot AS. 2006. Comparative Hazard Assessment of Imidacloprid and Carbaryl in the Context of Use for Burrowing Shrimp Control in Western Washington Estuaries. Department of Entomology, Washington State University, Richland, WA.